Received: 31 March 2016 | Revised: 2 June 2016 | Accepted: 10 June 2016

DOI 10.1002/qua.25192

TUTORIAL REVIEW

WILEY International Journal of QUANTUM CHEMISTRY

Classical and quantum dynamics at surfaces: Basic concepts from simple models

Matteo Bonfanti[1] | Rocco Martinazzo[1,2]

[1]Dipartimento di Chimica, Universitá degli Studi di Milano, 20133, Milano, Italy

[2]Istituto di Scienze e Tecnologie Molecolari, Consiglio Nazionale delle Richerche, 20133 Milano, Italy

Correspondence: Dipmartiento di Chimica, Universitá degli Studi di Milano, v. Golgi 19, 20133 Milano, Italy.
Email: rocco.martinazzo@unimi.it

Abstract

Elementary processes involving atomic and molecular species at surfaces are reviewed. The emphasis is on simple classical and quantum models that help to single out unifying dynamical themes and to identify the basic physical mechanisms that underlie the rich variety of phenomena of surface chemistry. Starting from an elementary description of the energy transfer between a gas-phase species and a surface—for both classical and quantum lattices—the key processes establishing the formation of an adsorbed phase (sticking, diffusion and vibrational relaxation) are discussed. This is instrumental for introducing the simplest chemical transformations involving adsorbed species and/or scattering of gas-phase molecules: Langmuir–Hinshelwood, Hot-Atom, and Eley–Rideal reactions forming complex molecules from elementary constituents, and dissociative chemisorption of molecules into smaller fragments. Applications are also provided illustrating the ideas developed along the way at work in real-world gas-surface problems.

KEYWORDS

gas-surface dynamics, surface scattering, Eley–Rideal, Hot-Atom, dissipative quantum dynamics

1 | INTRODUCTION

The dynamics of the atomic and molecular species interacting with solid surfaces plays an important role in several fields, from catalysis, electrochemistry, hydrogen economy, and green chemistry to atmospheric and interstellar chemistry. Heterogeneous catalysis is involved in about one-third of the modern economy and electrochemical processes employ charged surfaces and polarized interfaces. Surfaces measure biological evolution, and biological systems improve by ever increasing their interface-to-volume ratio.[1] The appearance of surfaces in the Universe, which occurred when the first generation of stars generated dust grains and "soot," is widely believed to be a key step in the chemistry and physics of the interstellar clouds that made formation of complex molecules possible.[2]

The theoretical understanding of the molecule-surface chemical bonding and of the microscopic dynamics of adsorption, diffusion, and reaction of adsorbates is of fundamental importance for modeling known processes, understanding new experimental data, predicting new phenomena, and controlling reaction pathways. This has become even more evident since the advent of two dimensional materials which, being "all-surface" systems, are particularly sensitive to the presence of any chemical species attached to them.[3] Microscopic (molecular) understanding of surface phenomena helps the new generation of materials scientists to design novel structures and to improve fabrication processes.[4] The importance of gas-surface interactions, though, is not limited to applications and concerns basic science, too. Fundamental questions remain open in the chemistry of the interstellar medium that involves the surface of the dust grains as a key ingredient. And, in this case, theoretical modeling is the only viable route to obtain reliable data, since experimental information on the interstellar chemistry is rather scarce and indirect.

In this review, we present a theoretical overview of the basic dynamical processes that may occur at the gas–solid interface. The focus is on elementary steps, and on simple classical and quantum models that have been developed over the years to understand surface phenomena and rationalize experimental findings. We keep the level of the discussion as simple as possible, and limit ourselves to general concepts and ideas, rather than diving in the abundant, often debated, literature of specific surface phenomena.

We start investigating energy transfer between a particle and a surface, a key issue in dynamics which determines the fate of the atoms or molecules impinging on the surface, i.e. whether they will be scattered back to the gas-phase or get trapped on the surface. We describe mechanical energy transfer using both classical and quantum lattice models, single out key factors, and establish general trends

MATTEO BONFANTI is currently post-doctoral research fellow with Prof. Rocco Martinazzo. After completing his PhD at the Università degli Studi di Milano in 2012, he worked in the Theoretical Chemistry Group of Leiden University with Prof. Geert-Jan Kroes. His main scientific interests include the modeling of processes at the gas-surface interface and the numerical methods of quantum dynamics, with a particular focus on quantum dissipative systems.

ROCCO MARTINAZZO works as Associate Professor at the Università degli Studi di Milano, Italy, where he received a PhD degree in 2002 and served his postdoctoral fellowship in the period from 2002 to 2004. He is head of the Chemical Dynamics Theory Group and conducts his research activity in theoretical chemistry, with focus on molecular processes in simple and complex media, dissipative and decoherent dynamics, quantum transport, electronic structure, and transport properties in nanoscale systems.

governing the transfer process. This is followed by a brief account of electronic friction and related phenomena that occur when the substrate is a metal and has a continuum of gapless excitations available.

Energy transfer is instrumental to sticking which is discussed next, by means of simple but surprisingly accurate models. Accommodation occurs via vibrational relaxation, but typically does not lead to immobile species on the surface: depending on energy barriers and temperature, thermal diffusion is always possible and makes surfaces a lively environment for the adsorbed species.

The final goal of the discussion is chemical reactivity, which follows next. Here the focus is on the main elementary reaction mechanisms either forming or breaking bonds. We discuss direct Eley–Rideal and thermal Langmuir–Hinshelwood recombinations, along with the Hot-Atom mechanism which is a possible intermediate between the two extremes; and we give a brief introduction to the dissociative chemisorption of molecules at surfaces.

Finally, we conclude with a handful of applications and numerical results from classical and quantum simulations. The emphasis here is to show at work the main concepts developed along the way, rather than presenting a detailed account of any specific aspect of the dynamics of molecules at surfaces. As a consequence, the chosen literature has a rather limited (illustrative) scope, and just reflects the personal taste and expertise of the authors.

2 | ENERGY TRANSFER

We start from the simplest yet fundamental process: the energy exchange between a colliding particle and the surface. When the projectile, be it an atom, an ion or a molecule, reaches the proximity of a surface, the coupling with the electronic or nuclear degrees of freedom determines a loss of the collision energy. The amount of energy deposited on the surface influences the fate of the scattering particle, which may still escape from the substrate attraction or get trapped and subsequently relax on the surface. In this section, we provide an elementary overview of the basic energy loss channels and mechanisms for this process.

2.1. | Classical lattice

The mechanical energy transferred by a scattering particle to the surface phonons has been long studied, either with molecular beam experiments or theoretical simulations, and a great wealth of results exists for a variety of scatterers on metal surfaces: rare gas atoms or ions, atomic hydrogen, diatomics, and other small molecules.[5] The first realistic (many phonon) study dates back to the early work by Zwanzig,[6] who proposed a simple model consisting of a collinear collision with a one-dimensional chain of atoms (see Figure 1). This one dimensional description was later reconsidered by Adelman and Doll[7] who developed a more complete Generalized Langevin Equation (GLE) classical treatment of the problem. Here, we present some elementary approaches to the problem that—despite their simplicity—have proven to be particularly useful in interpreting the experiments. For a more detailed review of these concepts, we refer to the work by Harris[5] and to some illuminating reports on atom/molecule-surface scattering experiments.[8]

We start from the one-dimensional chain by Zwanzig, and we conceptually split the process into two consecutive events: first the projectile collides with the chain end and leaves an amount of energy to the "surface atom" (the first atom of the chain). Then, this excitation leaves the surface and travels along the semi-infinite chain. To estimate energy transfer, it is thus necessary to consider the first collision and develop a plausible kinematic description of this event. We begin with a purely classical examination of the one-dimensional case, and later extend it to consider additional factors: off normal incidence, surface temperature, quantum nature of the phonon coordinates.

When the collision is much faster than the vibrational period of the surface atoms, *i.e.* $\omega_S \tau_c \ll 1$ (where ω_S is the surface atom frequency and τ_c the collision time), it is reasonable to assume that the collision is impulsive, a limit in which both linear momentum and mechanical energy are conserved quantities and the equations of motion can be exactly integrated. The scattering event is particularly simple in the center-of-mass (COM) reference frame of the binary system, i.e. with the help of the center of mass V and of the relative velocity of the two particles v,

$$V = \frac{m_S v_S + m_P v_P}{m_S + m_P} \tag{1}$$

$$v = v_P - v_S \tag{2}$$

v_P and v_S being the projectile and surface particle velocities in the laboratory frame, respectively, and m_P and m_S the corresponding masses. Indeed, as a consequence of energy and momentum conservation, the collision does not alter the velocity of the center of mass and simply reverts the relative velocity,

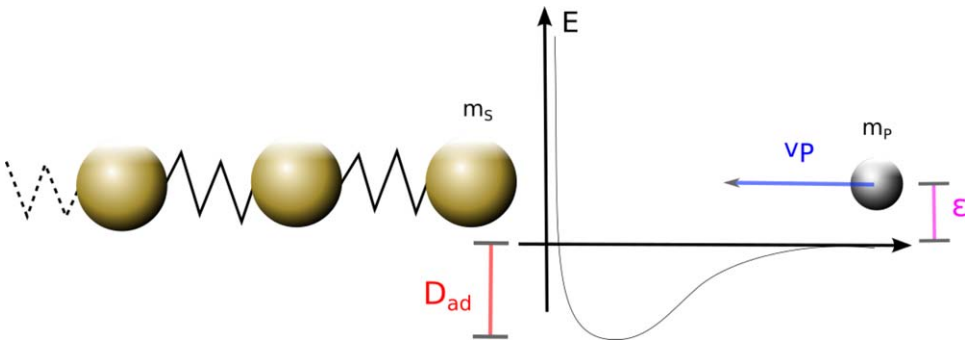

FIGURE 1 One dimensional chain model for investigating mechanical energy transfer and sticking in the adatom scattering off surfaces

$$v_S' = V' - \frac{m_P}{m_S+m_P}v' = V + \frac{m_P}{m_S+m_P}v = \frac{(m_S-m_P)v_S+2m_Pv_P}{m_S+m_P} \quad (3)$$

$$v_p' = V' + \frac{m_S}{m_S+m_P}v' = V - \frac{m_S}{m_S+m_P}v = \frac{(m_P-m_S)v_P+2m_Sv_S}{m_S+m_P} \quad (4)$$

where we used unprimed and primed letters to indicate pre- and post-collisional quantities, respectively.

Without any loss of generality, we first assume that the surface atom is initially at rest. As a consequence, v_P becomes also the velocity of the projectile relative to the target atom. Under this assumption, we can easily obtain that the final energy of the surface atom—which identifies with the energy transferred from the projectile atom—is given by

$$\delta\varepsilon = 4\,\frac{\alpha}{(1+\alpha)^2}\,\varepsilon \quad (5)$$

where $\alpha = m_P/m_S$ is the mass ratio and ε is the collision energy. This equation is commonly known as the "Baule" formula.[5] When the projectile is lighter than the target, the fraction of exchanged energy grows monotonically up to a complete transfer when the two masses are equivalent. Beyond this optimal value, according to *Eq.* 5, $\delta\varepsilon$ decreases with increasing ratio of the masses, but the model goes beyond its limits of validity. Indeed, when the projectile is heavier than the surface atom, its motion is *not* inverted by the collision and its final velocity $v_P' = (m_P-m_S)/(m_S+m_P)v_P$ still points toward the surface. This is the regime where multiple collisions occur and cannot be captured by the (binary) model above, unless the interaction of the surface atom with the rest of the chain is taken into account.

One simple variant of the Baule model is commonly used, in which it is assumed that the impulsive collision is preceded by an acceleration of the projectile due to an interaction with the substrate. In light of this consideration, the collision energy ε is increased by an amount D_{ad}, the adsorption energy,

$$\delta\varepsilon = \frac{4\alpha}{(1+\alpha)^2}\,(\varepsilon + D_{ad}) \quad (6)$$

This formula is referred to as "modified" or "attractive" Baule model. With respect to *Eq.* 5 it has a highly desirable property: in the limit of a zero collision velocity, an amount of energy is still transferred to the surface and thus it is possible to describe the trapping of the incident particle (an aspect which will be examined in detail in the following).

Harris[5] carried out an interesting analysis by comparing the results of explicit 1D chain simulations with the two limits of Eqs. 5 and 6. For a choice of the parameters which was relevant for scattering experiments, he showed that the actual energy transfer is intermediate between the predictions of the Baule and the modified Baule formulas. It is then reasonable to assume that for a single collision of a structureless particle the actual energy transfer is bounded from below by *Eq.* 5 and from above by *Eq.* 6. As the collision becomes faster—because of a higher collision energy or of a stronger interaction with the surface—the energy transfer tends toward the true impulsive limit, *Eq.* 5.

When lateral displacement is taken into account, different modelistic choices have been made in the past. As far as we are interested in the dependence of the energy transfer (or of any other quantity) on the *incidence angle*, we can assume a simple scaling relation. For instance, when the collision energy is small the projectile experiences a modest surface corrugation, and the linear momentum parallel to the surface is approximately a conserved quantity. This leads to normal energy scaling, i.e. the amount of transferred energy is proportional to the normal component of the incidence energy ($\varepsilon_\perp = \varepsilon\cos^2\theta$), as it is assumed, for example, in the so-called *hard-cube model*.[9] However, real surfaces can show a degree of corrugation, depending on many factors. Heuristically, it has been found that deviations from normal energy scaling are often comprised by a more general cosine scaling on $\varepsilon\cos^n\theta$ with $n \leq 2$. The opposite limit $n = 0$ corresponds to total energy scaling, which is usually an indication of a complex interaction with the surface that causes energy to be randomized prior to collision, e.g. because of partial trapping of the projectile.

Alternatively, the dependence of the energy transfer on the scattering angle can be captured by a binary collision model analogous to the one described above for collinear collisions. This is the strong corrugation limit where the impact of the (high energy) projectile with the surface effectively becomes a binary collision between the projectile and one of the surface atoms. The collision event is in the impulsive limit and can be handled similarly to above but now taking the full dimensionality of the problem into account. Specifically, the COM velocity and the magnitude of the relative velocity are left unchanged by the collision but now the post-collisional velocity $\mathbf{v}'$ can make an angle χ (the COM scattering angle) with the initial velocity vector $\mathbf{v}$, and the amount of energy transferred to the surface atom depends on χ as well. In the most common situation where $\alpha < 1$, χ uniquely fixes

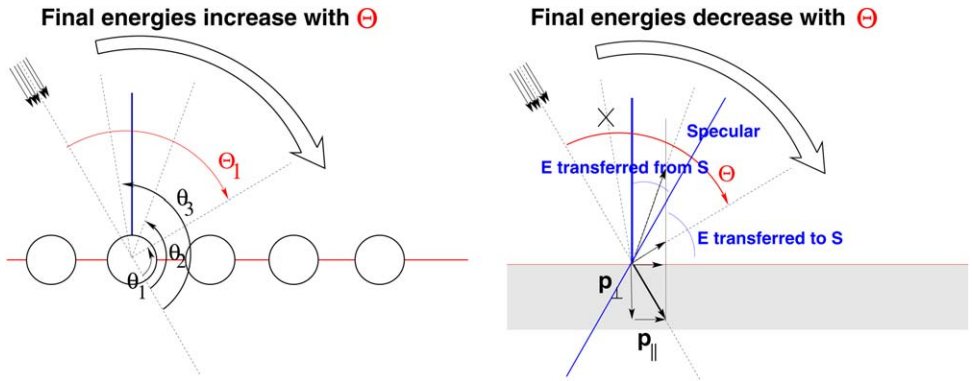

FIGURE 2 Schematics representing the energy distribution of the scattered projectiles in two different dynamical limits. Left: in the strong corrugation limit the exit energy increases with increasing Θ (the scattering angle as traditionally defined in surface scattering experiments). Also indicated the scattering angle θ of the binary collision. Right: in the flat surface limit the exit energy decreases with Θ and the sign of the energy transfer changes in going from sub to super specular directions

the scattering angle θ of the projectile velocity in the laboratory frame, i.e. the angle between $\mathbf{v}_P'$ and $\mathbf{v}_P$, and the energy transfer can be given as

$$\delta\varepsilon = 2\frac{\alpha}{(1+\alpha)^2}\left[1-\cos\theta\sqrt{1-\alpha^2\sin^2\theta}+\alpha\sin^2\theta\right]\varepsilon \tag{7}$$

Equation 7 extends the Baule formula to an arbitrary scattering angle. When $\theta=\pi$ the direction of the projectile velocity is inverted and the fraction of energy deposited on the surface takes the same value predicted by the Baule formula. However, $\delta\varepsilon$ decreases at decreasing values of θ and is zero for forward scattering ($\theta = 0$), i.e. when the projectile dives into the surface (and likely collides with some sub-surface atom). Hence, in an atom-surface experiment, if such a strongly corrugated limit holds, projectiles which are directly scattered by the surface are expected to have increasingly more (less) energy when moving toward super- (sub-) specular directions. This is in sharp contrast with the predictions one can make in the flat surface limit, where conservation of parallel momentum forces the projectile to emerge in a super-specular direction when it transfers energy to the surface, and sub-specular scattering is only possible if the projectile *gains* energy from the surface (see Figure 2). Traditionally, in atom-surface scattering experiments one identifies $\Theta=\pi-\theta$ as the "scattering" angle, and thus, in the above formula, the square root comes with the opposite sign if θ is replaced with Θ.

One interesting prediction of the model is the existence of a maximum scattering angle when the projectile is heavier than the target ($\alpha>1$). In this case, the square root in *Eq.* 7 limits the allowed values of θ around the forward direction ($|\theta| \leq \arcsin\frac{1}{\alpha}$), a phenomenon that a billiard player may experience when hitting the wrong balls. In such a situation, for each value of the scattering angle θ there exist two different values of the COM angle χ, corresponding respectively to near-forward ($\chi \approx 0$) and to near-backward ($\chi \approx \pi$) collisions in the COM frame: in the first case the ensuing energy transfer is still given by Eq. 7, while in the second case $\delta\varepsilon$ is obtained from *Eq.* 7 upon changing the sign in front of the square root (both cases appear forward-like in the laboratory frame, and cannot be distinguished on the basis of θ alone).

All the models described above assume a surface at a classical temperature of 0 K, i.e. with the surface atoms fixed at their equilibrium position before the collision. However, a rough qualitative dependence on surface temperature can be simply included by solving the problem with an explicit initial velocity of the surface atom v_S and then averaging the expression over a canonical distribution. In detail, from *Eq.* 3 we can compute the energy gained by the surface atom after the collision

$$\delta\varepsilon=\frac{1}{2}m_S v_S'^2-\frac{1}{2}m_S v_S^2=2\mu Vv=\frac{4\alpha(\varepsilon+D_{ad}-\frac{1}{2}m_S v_S^2)+2m_P(1-\alpha)v_S v_P}{(1+\alpha)^2} \tag{8}$$

and average over the thermal equilibrium distribution of the velocities v_S

$$\delta\varepsilon=\frac{4\alpha\left(\varepsilon+D_{ad}-\langle\frac{1}{2}m_S v_S^2\rangle\right)}{(1+\alpha)^2}=\frac{4\alpha}{(1+\alpha)^2}\left(\varepsilon+D_{ad}-\frac{1}{2}k_B T\right) \tag{9}$$

Even if *Eq.* 9 does not compare quantitatively with scattering experiments, it gives an useful indication on what is expected at finite temperatures: the energy transfer is reduced and this decrease scales linearly with the temperature. Interestingly, the averaging procedure above can be used also to capture the effect of quantum fluctuations of the surface in a simple quasi-classical model: the expression for $\langle v_S^2\rangle$ coming from classical equipartition needs only to be replaced with the appropriate quadratic deviation, *e.g.* $\langle v_S^2\rangle=\frac{\hbar\omega_S}{2m_S}$ for an harmonic oscillator of frequency ω_S.

When the scattering of molecules is considered, the presence of internal and rotational degrees of freedom often severely limits the success of the models based on the impulsive assumption. However, Baule formulas still give an extremely useful reference even in the case of failure, when their breakdown may give a clear indication on the active mechanisms. Just to mention two recent examples (among many), we refer to some recent experimental work on NO scattering from Au(111)[10] and a theoretical study on methane scattering from Ni (100) and Ni(111).[11]

2.2. | Quantum lattice

In the limit of low temperatures and/or light substrates, the quantum nature of the surface cannot be disregarded and the description of the

energy transfer due to collisions gets unavoidably more complicated. To get the feeling with the relevant physics we adopt a mixed quantum-classical description whereby the surface atom is treated quantally as a harmonic oscillator of frequency ω_S and the projectile is described classically and only weakly influenced by the interaction with the surface. The projectile is assumed to couple linearly with the surface atom coordinate q, $V(q)=-F(t)q$, along some pre-defined trajectory which determines the force $F(t)$ ($F(t)\to 0$ when $t\to\pm\infty$ for a scattering trajectory). The resulting model is analytically solvable and is known as the Forced Oscillator Model.[12,13] Its Hamiltonian takes the simple form

$$H=\hbar\omega_S\left(a^\dagger a+\frac{1}{2}\right)-\hbar f(t)(a^\dagger+a)=H_0+V(t)\quad V(t)=-\hbar f(t)(a^\dagger+a)$$

where $a^\dagger=\frac{q}{2\Delta q}-i\frac{p}{2\Delta p}$ ($a=\frac{q}{2\Delta q}+i\frac{p}{2\Delta p}$) is the usual raising (lowering) operator, $\hbar f(t)=F(t)\Delta q$ is the scaled force and the fundamental widths are $\Delta q=\sqrt{\hbar/2m_S\omega_S}$ and $\Delta p=\hbar/2\Delta q$. The dynamical problem is best solved in the interaction picture

$$i\hbar\frac{d|\Psi_I(t)\rangle}{dt}=V_I(t)|\Psi_I(t)\rangle$$

where the interaction-picture coupling potential

$$V_I(t)=e^{-\frac{i}{\hbar}H_0t}V(t)e^{+\frac{i}{\hbar}H_0t}=-\hbar f(t)(a_I(t)+a_I^\dagger(t))$$

is readily available from the well-known dynamical evolution of the free HO, $a_I(t)\equiv ae^{-i\omega_St}$. Indeed, the Baker–Haussdorf identity[14]

$$e^{A+B}=e^Ae^Be^{-\frac{1}{2}[A,B]} \tag{10}$$

(that holds for arbitrary operators A and B such that $[A,[A,B]]=[B,[A,B]]=0$) allows one to write the following identity ($\alpha,\beta\in\mathbb{C}$)

$$e^{\alpha a+\beta a^\dagger}=e^{\alpha a}e^{\beta a^\dagger}e^{-\frac{1}{2}\alpha\beta}=e^{\beta a^\dagger}e^{\alpha a}e^{+\frac{1}{2}\alpha\beta} \tag{11}$$

and, together with

$$e^{\alpha a}(a^\dagger)^n=(\alpha+a^\dagger)^ne^{\alpha a}\quad n\in\mathbb{N} \tag{12}$$

to prove that the operator

$$V(t)=e^{\alpha(t)a+\beta(t)a^\dagger+\Phi(t)},\quad \Phi(t)=\frac{1}{2}\int^t\left(\dot\alpha(\tau)\beta(\tau)-\alpha(\tau)\dot\beta(\tau)\right)d\tau$$

is such that

$$\frac{dV}{dt}=\left(\dot\alpha a+\dot\beta a^\dagger\right)V$$

One then sees that the Schrödinger equation

$$|\Psi_I(t)\rangle=U_I(t,t_0)|\Psi_I(t_0)\rangle$$

is solved by the following time-evolution operator

$$U_I(t,t_0)=\exp\left[i\left(g^*(t,t_0)a+g(t,t_0)a^\dagger+\phi(t,t_0)\right)\right]$$

where

$$g(t,t_0)=\int_{t_0}^t f(\tau)e^{i\omega_S\tau}d\tau,\quad \phi(t,t_0)$$
$$=\int_{[t,t_0]\times[t,t_0]}f(\tau_1)f(\tau_2)\Theta(\tau_1-\tau_2)\sin\left[\omega_S(\tau_1-\tau_2)\right]d\tau_1d\tau_2$$

and Θ is the usual Heaviside (or step) function, $\Theta(x)=1$ for $x\geq 0$ and zero otherwise.

Of major interest is the probability amplitude ψ that the HO makes a transition $n\to m$ in the limit where the system is prepared in the infinite past in n ($t_0\to-\infty$) and probed in the infinite future in m ($t\to+\infty$), i.e. $\psi(m\leftarrow n)=\langle m|U_I(+\infty,-\infty)|n\rangle$. Using the identities of *Eqs.* 11 *and* 12, and the standard expression

$$|n\rangle=\frac{(a^\dagger)^n}{\sqrt{n!}}|0\rangle$$

one finally arrives at

$$\psi(m\leftarrow n)=\frac{e^{i\Phi}}{\sqrt{m!n!}}\exp\left(-\frac{|\tilde f_S|^2}{2}\right)\langle 0|(i\tilde f_S+a)^m(i\tilde f_S^*+a^\dagger)^n|0\rangle$$

where $\Phi=\phi(+\infty,-\infty)$, $\tilde f_S$ is the Fourier transform of the (scaled) external force evaluated at the HO frequency

$$\hat f(\omega)=\int_{-\infty}^{+\infty}f(t)e^{i\omega t}dt\quad \tilde f_S=\hat f(\omega_S)$$

and

$$\langle 0|(+i\tilde f_S+a)^m(i\tilde f_S^*+a^\dagger)^n|0\rangle=m!n!\begin{cases}i^{m-n}(\tilde f_S^*)^{m-n}\sum_{k=0}^{n}\frac{(-)^k|\tilde f_S|^{2k}}{(n-k)!k!(m-n-k)!} & m\geq n\\ i^{n-m}(\tilde f_S)^{n-m}\sum_{k=0}^{m}\frac{(-)^k|\tilde f_S|^{2k}}{(m-k)!k!(n-m-k)!} & m<n\end{cases}$$

It follows, for instance, that excitation from the ground-state occurs according to a Poisson distribution (we now use n to label the final state)

$$P(n\leftarrow 0)=\frac{|\tilde f_S|^{2n}}{n!}e^{-|\tilde f_S|^2}$$

where $\tilde f_S$ determines both the average excitation number (number of phonons) and the width of the distribution through

$$\langle n\rangle=\langle\Delta n^2\rangle=|\tilde f_S|^2=\frac{1}{2m_S\hbar\omega_S}\left|\int_{-\infty}^{+\infty}F(t)e^{i\omega_St}dt\right|^2$$

Of interest is the impulsive limit considered above, where $F(t)$ is sharply peaked around the time t_0 of the collision, $F(t)\approx I_0\delta(t-t_0)$, and I_0 is the momentum change, $I_0=2m_Pv_P/(1+\alpha)$. In this limit the resulting average energy transferred to the HO reads as

$$\delta\varepsilon=\hbar\omega_S\langle n\rangle=\frac{I_0^2}{2m_S}=\frac{4\alpha}{(1+\alpha)^2}\varepsilon$$

i.e. just the classical Baule result of *Eq*. 5. As noticed above, though, this impulsive limit only attains at energies high enough that $\tau_c\omega_S \ll 1$ holds, where τ_c is the collision time. Using Δq as relevant length scale of the interaction (i.e., $\Delta q = v_P\tau_c$), this condition thus implies $\varepsilon \gg \alpha\hbar\omega/4$, i.e.

$$\langle n\rangle \gg \frac{\alpha^2}{(1+\alpha)^2}$$

This means that, unless the projectile is much lighter than the target (e.g., electrons), the collisional transfer of energy in this impulsive limit is always in the classical regime for the HO too (i.e., $\langle n\rangle \gg 1$ and $P(n \leftarrow 0)$ reduces to a Gaussian).

In a more realistic situation, the projectile interacts with a surface atom that, in turn, interacts with the rest of the substrate. A more appropriate forced oscillator model is thus

$$H=\sum_k\left(\frac{p_k^2}{2m_k}+\frac{m_k\omega_k^2q_k^2}{2}\right)-q_SF\quad q_S=\sum_k c_kq_k$$

where q_k (p_k) are normal mode—or phonon—coordinates (momenta), ω_k their frequencies, q_S is the displacement of the surface atom from its equilibrium position and c_k are numerical coefficients which describe the normal mode transformation. Using the above results the problem is readily solved by replacing F with Fc_k for each normal mode oscillator, and this allows one to define the probability density that the k-th oscillator gains the energy ε

$$\rho_k(\varepsilon)=\sum_n p_n^{(k)}\delta(\varepsilon-n\hbar\omega_k)$$

where $p_n^{(k)}=|\langle n\rangle_k|^n\exp(-|\langle n\rangle_k|)/n!$ and $\langle n\rangle_k=|c_k|^2|\tilde{F}(\omega_k)|^2/2m_k\hbar\omega_k$. Finding the statistical distribution governing the *total* energy transferred to the surface becomes thus a standard statistical problem involving uncorrelated variables, which only requires calculation of the (fundamental) characteristic functions associated to the above probability densities $\rho_k(\varepsilon)$. The solution can be written as

$$\rho(\varepsilon)=\frac{1}{2\pi}\int_{-\infty}^{+\infty}\exp\left[-i\varepsilon\tau+\int_0^\infty\pi_1(\omega)(e^{i\hbar\omega\tau}-1)d\omega\right]d\tau$$

where $\pi_1(\omega)$ reads as

$$\pi_1(\omega)=|\tilde{F}(\omega)|^2I(\omega),\quad I(\omega)=\sum_k\frac{|c_k|^2}{2m_k\hbar\omega_k}\delta(\omega-\omega_k)$$

and is the overall *one-phonon* probability distribution. $\pi_1(\omega)$ alone determines the total energy transferred to the lattice during the collision and is a measure of both the strength of the force $|\tilde{F}(\omega)|^2$ and the "density of the coupling" $I(\omega)$ between the surface atom and its environment. The limit of $\pi_1(\omega)$ "small" gives $\rho(\varepsilon)\approx P_{el}\delta(\varepsilon)+\pi_1(\varepsilon/\hbar)$ and describes a transfer of energy that only occurs through single excitation of the surface oscillators. Interestingly, in this case, the elastic probability P_{el} reads as

$$P_{el}=\exp\left(-\int_0^\infty\pi_1(\omega)d\omega\right)=e^{-W}$$

where, in the impulsive limit considered above ($F(t)\approx I_0\delta(t-t_0)$), W takes a Debye–Waller-like form, $W\approx I_0\Delta q^2/\hbar^2$.

2.3 | Electronic friction

When an atom or a molecule impinges on a *metal* surface there exists the possibility that the metal electrons are excited, and so-called electron–hole (e–h) pairs form. Such kind of excitation, obviously related to the particular electronic structure of metals and to their continuum of gapless excitations, forms an energy loss channel that may contribute to the overall energy transfer to the surface. This may be particularly important for light species which, according to *Eqs*. 5 *and* 6, exchange only a little amount of mechanical energy with the surface atoms. The effect may be even spectacular and lead to detectable chemical currents (*chemicurrents*), as it happens when energetic chemical processes take place on the surface of a metal substrate.[15] More generally, though, the effect of e–h pair excitations is rather difficult to ascertain, both theoretically and experimentally, and the field presently lacks of well-rounded and established concepts. The only unifying theme is that these phenomena are electronically non-adiabatic, and thus involve multi-state dynamics and non-radiative electronic transitions. Furthermore, the states involved in the process form a very dense set, and this typically prevents any attempt to directly manage them. This is in striking contrast with the non-adiabatic dynamics in the gas-phase where a handful of electronic states are needed at worst, and they can be accurately described with the help of adiabatic surfaces and non-adiabatic couplings between them (or, equivalently, diabatic states).

Actually, a kind of "molecular" non-adiabatic dynamics can also occur at metal surfaces, but it is considerably more complicated than in gas phase since it involves coupling to different continua: each molecular electronic state comes with the e–h continuum of the metal, and it is all but obvious whether "electronic excitations" primarily occur on the delocalized (i.e., metallic) states or the localized (i.e., molecular) ones or both. One paradigmatic test case of this kind is the scattering of vibrationally excited NO molecules off the Au(111) surface,[10,16–25] where both neutral (NO/Au) and negative ion (NO^-/Au^+) molecular states appear to be involved and coupled to the continuum of metal e–h excitations, resulting in a rather fast vibrational de-excitation of the projectile molecules. Rather elaborate theoretical models have been developed to explain the key experimental findings on this system,[16,19,21–25] and only recently a sound perspective emerged on the basis of classical, non-adiabatic molecular dynamics simulations using the impressive number of 10^{11} model adiabatic states in an independent electron transfer hopping method.[23,24] However, later experimental results have suggested that the agreement between theory and experiments may be fortuitous, thereby calling for a deeper understanding of the scattering process.[26] Interestingly, as long as only vibrational de-excitation is concerned, open-system quantum dynamical results including couplings to the e–h pairs at the Fermi-golden rule level but using a single potential energy surface (*i.e.*, without invoking any electron transfer) do reproduce the observed vibrational distribution of the scattered molecules.[25] For a more detailed account of the current status of the field we refer to the excellent review article by Golibrzuch et al.[26]

Barring these "pathological" cases, in typical situations only electronic excitations between delocalized states of the metal substrate are involved, and these have little effects on the adsorbate-substrate energetics: adsorption profiles for different levels of excitation are expected to be almost identical to each other, just shifted in energy to account for their different energy content. Their presence, though, does affect the

adsorbate dynamics, because the possible energy loss into electronic excitations: the metal electrons act like a "bath" that is able to exchange energy with the atomic or molecular species we are interested in. In such situations, there is no need to abandon the electronic *adiabatic* picture of the dynamics, since one can subsume the role of the "electronic reservoir" into dissipative effects on the dynamics. This is the molecular dynamics with electronic friction[27] approach, whereby a frictional force is introduced in the equations of motion along with the appropriate accompanying random force. The approach is meaningful only when the *classical* description of particle dynamics is possible, but can make use of accurate information on the electronics. The electronic friction coefficient subsumes the response of the electronic bath to the particle dynamics, and can be computed from *first-principles*. It is necessarily state-dependent: the effect of the metal substrate on the particle dynamics cannot be the same if the particle is far from or close to the surface.

Even though rigorous formulations of the electronic friction effect may be intricate, the main ideas can be easily understood already at a classical level: particle dynamics induces electric fields into the metal and sets free electrons in motion, which then undergo Ohmic damping. The effect of the induced fields is best seen with a related physical problem, that of a charged particle forced to move with constant velocity $\mathbf{v}$ in a metal substrate.[28] The particle, of charge $Z|e|$ and mass m, creates a total electric field $\mathbf{E}(\mathbf{r},t)=\mathbf{E}_{\text{ext}}(\mathbf{r},t)+\mathbf{E}_{\text{int}}(\mathbf{r},t)$, which is the sum of the bare field due to the charge $\mathbf{E}_{\text{ext}}(\mathbf{r},t)$ and of a response field $\mathbf{E}_{\text{int}}(\mathbf{r},t)$. The rate of change of particle energy (i.e., the power that needs to be compensated by external forces if the particle has to keep its speed) is obtained from Lorentz law

$$\frac{d}{dt}\left(\frac{m\mathbf{v}^2}{2}\right)=\frac{dW}{dt}=Z|e|\,\mathbf{v}\cdot\mathbf{E}(\bar{\mathbf{r}}(t),t)$$

where $\bar{\mathbf{r}}(t)=\mathbf{r}_0+\mathbf{v}t$ is the particle trajectory (there is no need to worry about self-interaction effects since they do not contribute to the *rate* of change of the energy). The total field can be computed from the charge density $\rho_{\text{ext}}(\mathbf{r})=Z|e|\delta(\mathbf{r}-\bar{\mathbf{r}}(t))$ with the help of Maxwell's equations upon moving to $(\mathbf{k},\omega)$-space through space-time Fourier transforms, which we define according to

$$f(\mathbf{k},\omega)=\int_{\mathbb{R}^3}d^3\mathbf{r}\int_{-\infty}^{+\infty}dt\,e^{i(\omega t-\mathbf{kr})}f(\mathbf{r},t)$$

in such a way that $\nabla\to i\mathbf{k}$ and $\partial/\partial t\to -i\omega$ hold. Notice that for $f(\mathbf{r},t)$ real, a conjugation symmetry holds, namely $f^*(\mathbf{k},\omega)=f(-\mathbf{k},-\omega)$. The charge density is easily transformed to $\rho_{\text{ext}}(\mathbf{k},\omega)=2\pi Z|e|e^{-i\mathbf{k}\mathbf{r}_0}\delta(\omega-\mathbf{kv})$ and the field, in the approximation where it can be obtained from a scalar potential, is purely longitudinal (i.e., $\mathbf{E}(\mathbf{k},\omega)$ is parallel to $\mathbf{k}$) and follows directly from Gauss' law

$$\mathbf{E}(\mathbf{k},\omega)=-i\frac{4\pi}{k^2}\frac{\rho_{\text{ext}}(\mathbf{k},\omega)}{\varepsilon(\mathbf{k},\omega)}\mathbf{k}$$

where $\varepsilon(\mathbf{k},\omega)$ is the total dielectric permittivity of the substrate. Hence, upon taking conjugation symmetry into account, the required field reads as

$$\mathbf{E}(\bar{\mathbf{r}}(t),t)=\frac{Z|e|}{2\pi^2}\int_{\mathbb{R}^3}\frac{d^3\mathbf{k}}{k^2}\int_{-\infty}^{+\infty}d\omega\,\Im\left(\frac{1}{\varepsilon(\mathbf{k},\omega)}\right)\delta(\omega-\mathbf{kv})\mathbf{k}$$

and the power loss can be written as

$$-\frac{dW}{dt}=\frac{Z^2e^2}{\pi^2}\int_{\mathbb{R}^3}\frac{d^3\mathbf{k}}{k^2}\int_0^{\infty}d\omega\omega\,\Im\left(-\frac{1}{\varepsilon(\mathbf{k},\omega)}\right)\delta(\omega-\mathbf{kv})$$

where $\Im\varepsilon(\mathbf{k},\omega)\geq 0$, a general (thermodynamic) property of the dielectric permittivity, guarantees that the above expression corresponds to an energy loss (stopping power).[29,30] For isotropic media the above expression simplifies to

$$-\frac{dW}{dt}=\frac{2Z^2e^2}{\pi}\int_0^{\infty}d\omega\omega\int_{\omega/v}^{\infty}\frac{dk}{k}\,\Im\left(-\frac{1}{\varepsilon(k,\omega)}\right)$$

and can be evaluated using, e.g., the analytic expression of $\varepsilon(k,\omega)$ for a free-electron gas in the random phase approximation*.

From a different perspective, for slowly moving ions ($v\ll v_{\text{F}}$, where v_{F} is the Fermi velocity of the metal), the interaction with the electron sea can be seen as scattering of electrons at the Fermi surface off the (screened) potential of the static impurity ion, similarly to the impurity contribution to the resistivity of a metal. The energy loss per unit distance traveled in the medium, i.e. the frictional force acting on the ion, is found to be linear in v[31–33]

$$F_\eta=\frac{1}{v}\frac{dW}{dt}=-vv_{\text{F}}m_{\text{e}}n\sigma_{\text{t}}$$

where n is the density of the electron gas (taken to be homogeneous), m_{e} the electron mass and σ_{t} the transport cross section. The ensuing electron friction coefficient, $\eta=v_{\text{F}}m_{\text{e}}n\sigma_{\text{t}}$, can be given in terms of scattering phase-shifts at the Fermi energy

$$\eta=\frac{4\pi\hbar^2m_{\text{e}}n}{v_{\text{F}}}\sum_{l=0}^{\infty}(l+1)\sin^2(\delta_l(k_{\text{F}})-\delta_{l+1}(k_{\text{F}}))$$

and can be computed *ab initio* using the Khon–Sham eigenstates for the impurity problem in a homogeneous gas at any desired density. This self-consistent approach to the stopping power remedies for the deficiencies of the linear response theory—*e.g.* it correctly describes the appearance of bound states in the (screened) impurity potential that occurs when screening is not efficient enough (small n)—and provides a simple, "local" recipe to estimate the electronic friction coefficient for neutrals (the local density friction approximation, LDFA).[34,35]

3 | STICKING

When an incident particle, which is subjected to an attractive interaction with the surface, loses some energy, there is the possibility that the remaining kinetic energy may not be enough to escape from the

* The random phase approximation partially accounts for electron–electron interactions, in the sense that it includes them at the mean-field (Hartree) level. To be specific, in the exact expression that gives ε in terms of the so-called irreducible polarizability Π (the density response to variations in the *total* electric potential), namely $\varepsilon(k,\omega)=1-\frac{4\pi e^2}{k^2}\Pi(k,\omega)$, one replaces $\Pi(k,\omega)$ with the independent-particle density response in the mean-field system, $\chi_0(k,\omega)$. If the uniform electron gas is treated at the Hartree level, the one-particle states are plane-waves, the one-electron levels are free-particle energies, and χ_0 reads, in the collisionless limit, as $\chi_0(q,\omega)=-\frac{e^2}{4\pi^3}\int d^3\mathbf{k}\frac{f(\mathbf{k}-\mathbf{q}/2)-f(\mathbf{k}+\mathbf{q}/2)}{\hbar^2\mathbf{kq}/m_{\text{e}}+\hbar\omega}$, where $f(\mathbf{k})$ is the Fermi–Dirac occupation function for a free-electron at energy $\hbar^2\mathbf{k}^2/2m_{\text{e}}$.

adsorption well. At short time the adsorbed species is metastable and this process is referred to as trapping. The name sticking is more appropriately used when the excess energy is completely dissipated to the surface and thermal equilibrium is achieved.

A simple analytical model of the sticking dynamics is obtained using the same assumptions we used above to estimate the energy transfer (Figure 1). We consider an incident atom of mass m_P and kinetic energy ε that approaches a surface in the perpendicular direction. When the projectile is close to the surface it gets accelerated by the attractive potential, an effective well of depth D_{ad}, and then collides with one of the surface atoms losing an amount of energy equal to $\delta\varepsilon$. Soon after collision has occurred, the surface atom rapidly dissipates its energy to the lattice through mass-matching collisions and comes to rest. If the collision is much faster than the time scale of the surface vibrational motion, the collision dynamics can be considered impulsive and $\delta\varepsilon$ can be estimated with the modified Baule formula, *Eq*. 6. Note the use of standard Baule formula would not be justified in this context, since an adsorption interaction needs to be explicitly considered in the case of sticking and the use of *Eq*. 5 would lead to inconsistent conclusions, such as a zero sticking probability in the limit $\varepsilon \to 0$. The post-collision energy $\varepsilon' = \varepsilon - \delta\varepsilon$ is the energy relevant for trapping to occur, i.e. $\varepsilon' < 0$ is the appropriate trapping condition. Using *Eq*. 6 under this condition we obtain

$$\varepsilon < \frac{4\alpha}{(1-\alpha)^2} D_{ad} = \varepsilon_{th} \tag{13}$$

Thus this model predicts the existence of a threshold energy to sticking which depends on the mass ratio α and the depth of the adsorption well D_{ad}.

This crude description predicts that the sticking probability P_s is a simple step function centered at the threshold value, $P_s(\varepsilon) = \Theta(\varepsilon_{th} - \varepsilon)$. However, realistic sticking probability curves show some broadening around ε_{th} and are effectively less than 1 (greater than zero) for energies slightly below (above) ε_{th}. Clearly, this is due to the thermal agitation of the surface atoms, an effect that can be captured already in the impulsive limit discussed above. Specifically, when the surface atom moves with velocity v_S, the trapping condition $\delta\varepsilon > \varepsilon$, with $\delta\varepsilon$ given by *Eq*. 8, determines the values of v_S that allow the projectile to get trapped in the adsorption well, for each value of ε,

$$v_S \in \mathcal{I}(\varepsilon) \equiv [v_-, v_+], \quad v_\pm = -\frac{1-\alpha}{2}\sqrt{\frac{2(\varepsilon + D_{ad})}{m_P}} \pm \frac{1+\alpha}{2}\sqrt{\frac{2D_{ad}}{m_P}} \tag{14}$$

Since trapping does occur with certainty for $v_S \in \mathcal{I}(\varepsilon)$, the sticking probability is obtained by integrating the distribution of surface atom velocities over this interval

$$P_s(\varepsilon) = \int_{\mathcal{I}(\varepsilon)} g(v)dv \tag{15}$$

where

$$g(v) = \left(\frac{m_S}{2\pi k_B T}\right)^{1/2} e^{-\frac{m_S u^2}{2k_B T}}$$

is the Maxwell–Boltzmann distribution appropriate for a classical "target." Notice that the range of relevant velocities is centered around a value that optimizes the energy transfer, as can be readily seen with the help of *Eq*. 3: for $v_S = -(1-\alpha)\sqrt{(\varepsilon + D_{ad})/2m_P}$ the post-collisional velocity of the projectile vanishes, i.e. the surface atom stops the projectile.

When adsorption is activated, the model presented above requires some adjustment to account for the presence of a barrier, and its contrasting effects. An energy barrier E_b in the adsorption profile limits the access of the projectile into the adsorption region but, on the other hand, increases the desorption threshold and makes trapping easier. Thus, the barrier introduces a *crossing condition* and modifies the above trapping condition into $\varepsilon' < E_b$. We assume that the energy barrier E_b is in the relative motion of the projectile w.r.t. the surface atom and, for definiteness, that the projectile atom travels toward the surface (leftward). Then, for each given ε the barrier-crossing condition requires that the kinetic energy in the *relative* coordinate exceeds E_b, or equivalently

$$v_S \geq v_{th}(\varepsilon) \equiv -v_P(\varepsilon) + \sqrt{\frac{2(1+\alpha)E_b}{m_P}} \tag{16}$$

where $v_P = \sqrt{2\varepsilon/m_P}$ is the projectile speed. The modified trapping condition, on the other hand, leads to

$$v_S \in \mathcal{I}(\varepsilon) \equiv [v_-, v_+], \quad v_\pm = -\frac{1-\alpha}{2}\sqrt{\frac{2(\varepsilon + D_{ad})}{m_P}} \pm \frac{1+\alpha}{2}\sqrt{\frac{2(D_{ad} + E_b)}{m_P}}$$

In turn, the sticking probability takes the same form of *Eq*. 15, but with a different integration domain, $\mathcal{I}(\varepsilon) \to \mathcal{I}(\varepsilon) \cap [v_{th}(\varepsilon), +\infty)$ (see Figure 3).

A word of caution is necessary on the presence of multiple collision events, since they are predicted for both the non-activated and activated models when $v_S < -(1-\alpha)v_P/2$. In these conditions, additional trapping might occur beyond the "direct trapping" window $v_S \in [v_-, v_+]$: when $v_S < v_-$ projectiles that are not trapped at the first bounce may dissipate the excess energy after a number of collisions. Trapping through multiple collisions is hardly captured by the simple arguments given above and its possible occurrence should always be born in mind.

Even if this impulsive sticking description might appear quite crude, it has proven to capture the essential physics of the process with the help of two system properties only, the height of the barrier E_b and the depth of the interaction well D_{ad}. These two parameters may either reflect the true energetics of the system or can be considered as effective adjustable parameters, which sum up dynamical effects in addition to the shape of the potential energy surface. The model can also be extended to capture the low temperature behavior of the surface, just by replacing $g(v)$ with the appropriate velocity distribution of the surface atom quantum oscillator, coupled to the rest of the lattice. As is shown in Appendix B of Ref. [36], the function $g_q(v)$ required in this case is given by

$$g_q(v) = \sqrt{\frac{m_S}{\pi\hbar\Omega_T}} e^{-\frac{m_S u^2}{\hbar\Omega_T}} \tag{17}$$

where the temperature-dependent effective frequency Ω_T accounts for the coupling with the bulk and is conveniently written in the form[36]

$$\Omega_T = \frac{\int_0^{+\infty} d\omega J(\omega)\omega^2 \coth\left(\frac{\hbar\omega}{2k_B T}\right)}{\int_0^{+\infty} d\omega J(\omega)\omega} \tag{18}$$

Here the function $J(\omega)$ is a so-called spectral density of the coupling (see Appendix): in this case it subsumes the coupling of a hypothetical

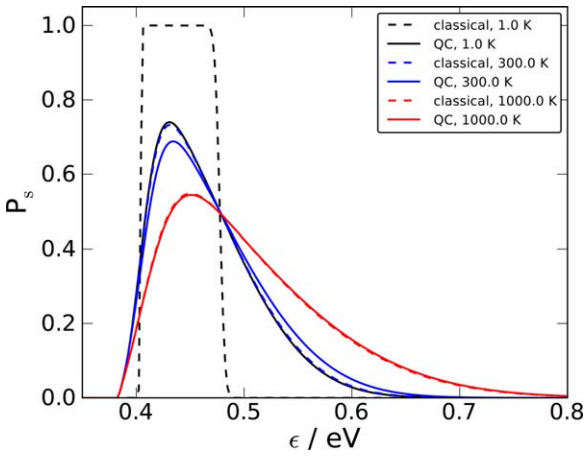

FIGURE 3 Sticking probabilities for an activated model system with $\alpha = 0.01$, $D_{ad} = 1.5$ eV and $E_b = 0.4$ eV, as obtained using Eq. 15. Results are shown for the Maxwell–Boltzmann (dashed lines) and for the quantum (solid lines) distribution of the velocities of the surface atom, at different temperatures (black, blue and red for $T = 1$, 300 and 1000 K, respectively). The surface atom frequency ω_S was set to 400 cm^{-1}

adsorbate that interacts bilinearly with the surface atom and in turn with the bulk (the identity of the adsorbate is irrelevant since the strength of the coupling factors out in the above ratio). In absence of coupling to the bulk, for instance, $J(\omega)$ reduces to a $\delta-$ peak centered around ω_S and Ω_T above only depends on the bare frequency of the oscillator.

The effective frequency Ω_T takes the lowest value in the $T = 0$ K limit,

$$\Omega_0 = \frac{\int_0^{+\infty} d\omega J(\omega)\omega^2}{\int_0^{+\infty} d\omega J(\omega)\omega} \tag{19}$$

and increases linearly with T at high temperatures,

$$\Omega_T \approx \frac{2k_B T}{\hbar} \tag{20}$$

provided the thermal energy is much larger than the zero point energy at the cutoff frequency of the phonon "bath" (the so-called Debye frequency ω_D), i.e. $k_B T \gg \hbar\omega_D/2$. In this limit, of course, $g_q(v)$ reduces to the classical Maxwell–Boltzmann distribution, irrespective of the coupling to the rest of the lattice.

4 | DIFFUSION

Once a particle has been adsorbed and equilibrated on the surface, diffusive motion sets in because of the energy fluctuations that the coupling to the lattice gives rise to. We shall assume that the surface presents a periodic arrangement of stable adsorption sites, separated by energy barriers E_d significantly smaller than the energy threshold for desorption. The adsorbate then typically moves on a corrugated potential energy profile and is subjected to energy dissipation and fluctuation due to its coupling with the surface phonon bath.[37]

In a discrete microscopic limit, we may think of a diffusing particle as a "random walker," a particle which jumps from one adsorption site to another with a well definite hopping probability.[38] Let l_w be the average step length and Γ_w^{-1} be the average time required for a step. If we take an ensemble of walkers, initially placed at $\mathbf{x}=0$, after N steps the average (squared) distance travelled by the walkers is

$$\langle \mathbf{x}_N^2 \rangle = \langle \sum_{k=1}^{N} \Delta \mathbf{x}_N^2 \rangle = \sum_{k=1}^{N} \langle \Delta \mathbf{x}_N^2 \rangle = N l_w^2 \tag{21}$$

where $\langle \Delta \mathbf{x}_k \Delta \mathbf{x}_j \rangle = \delta_{kj} l_w$ holds because the steps $\Delta \mathbf{x}_j$ are assumed to be uncorrelated. Since each step takes place in a time Γ_w^{-1}, $N = \Gamma_w t$ and we obtain

$$\langle \mathbf{x}_N^2 \rangle = l_w^2 \Gamma_w t \tag{22}$$

i.e., the average squared displacement scales linearly with time, and the constant of proportionality is given by microscopic quantities, the average step length l_w and the hopping rate Γ_w.

The same results is obtained when the opposite limit is assumed, i.e. when the dynamics is considered as a continuous process and the well known Fick's law $\mathbf{j} = -D\nabla f$ is used to "close" the continuity equation for the particle distribution density[†] $f(\mathbf{x}, t)$

$$\frac{\partial f}{\partial t}(\mathbf{x}, t) = -\nabla \mathbf{j} = D\nabla^2 f(\mathbf{x}, t) \tag{23}$$

Here D is the diffusion coefficient, and is directly related to the rate of variation of the squared displacement, as it follows from the chains of identities

$$\frac{d\langle \mathbf{x} \rangle_t^2}{dt} = \int \mathbf{x}^2 \frac{\partial f}{\partial t} d^v \mathbf{x} = D \int \mathbf{x}^2 \nabla^2 f d^v \mathbf{x} \equiv 2vD$$

where v is the dimensionality of the problem ($v = 2$ in our case). More generally, in realistic cases, only at long time the diffusive behavior sets in, and the diffusion coefficient is best defined as

$$D = \frac{1}{2v} \lim_{t \to \infty} \frac{d\langle \mathbf{x}(t)^2 \rangle_t}{dt} \tag{24}$$

where $\mathbf{x}(t)$ is a trajectory started at $\mathbf{x}(0) = \mathbf{0}$ and the average is taken over the equilibrium distribution of initial velocities and over the environmental variables.[‡] The diffusion coefficient is the fundamental quantity that characterizes the diffusion process, regardless of the details of the subsumed microscopic model of transport. It measures the ability of particles to spread over the surface and to offset any concentration gradient that may build on it, because of e.g. reactions or adsorption at specific locations. Under special circumstances, it may also happen that $D = 0$ and then the motion is at most subdiffusive, or $D = \infty$ and the motion is superdiffusive.[39]

[†] The corresponding quantity in random walk dynamics is $f_N(\mathbf{x})$, the probability that a walker is found in $\mathbf{x}$ after N steps; in particular, if the walkers are all started in $\mathbf{x} = \mathbf{0}$, $f_N(\mathbf{x})$ ($f(\mathbf{x}, t)$) is the fundamental transition probability that a walker makes a displacement $\mathbf{x}$ in N steps (in a time t). Noteworthy, since the steps are uncorrelated, $f_N(\mathbf{x})$ readily follows from $g(\mathbf{x}) = f_1(\mathbf{x})$, the one-step transition probability, and its characteristic function $\hat{g}(\mathbf{k}) = \langle \exp(i\mathbf{kx}) \rangle_g$. Specifically, in v dimensions it reads as $f_N(\mathbf{x}) = (2\pi)^{-v} \int \exp(-i\mathbf{kx}) [\hat{g}(\mathbf{k})]^N d^v \mathbf{k}$.

[‡] Depending on the adopted approach, this "environmental averaging" is either over the initial conditions of the phonon bath or over the realizations of the stochastic force it exerts on the system.

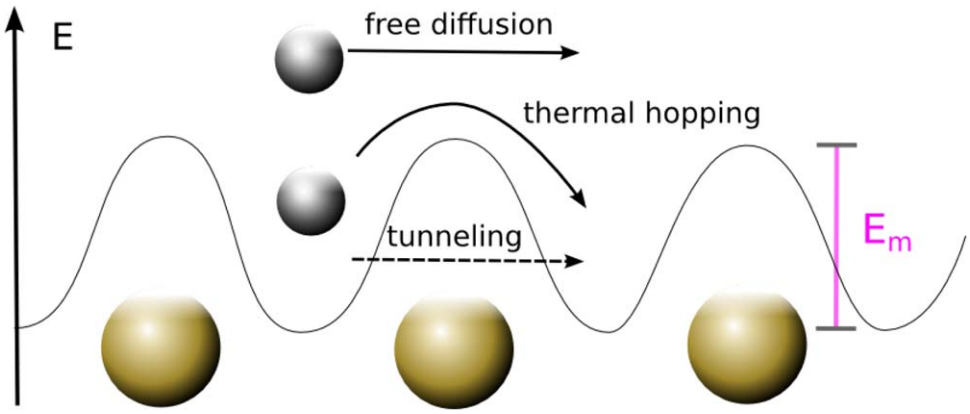

FIGURE 4 A schematics illustrating the different diffusion regimes discussed in the main text

We now address the problem of identifying the different dynamical regimes for diffusion and characterize D in terms of simple microscopic quantities (Figure 4). When the thermal energy k_BT is much larger than the energy of the diffusion barrier, the adsorbate moves essentially free on a flat surface. In this case, the surface potential plays no role except to prevent particle escape and the motion is free diffusion, similar to original Brown's observation.[40] We assume that for a variable time interval, the particle moves undisturbed with a constant velocity (i.e., ballistically). After this time, a collision takes place and the particle moves again uniformly but with a different velocity—randomly picked from the local equilibrium distribution—until the next collision. In this simplified description, the collisions are random events determining an exchange of energy between the adsorbate and the environment (the phonon bath of the surface in particular). If τ_c is the average time between collisions, dt/τ_c is the probability that a particle undergoes a collision in the time interval dt, and then the survival probability $P(t)$ that the particle travels for a time t after its last collision at $t = 0$ satisfies

$$P(t+dt)=P(t)\left(1-\frac{dt}{\tau_c}\right)$$

and takes the form

$$P(t)dt=e^{-t/\tau_c}\,dt \tag{25}$$

The time τ_c is indeed the average time between collisions, as can be readily seen by computing the collisional probability $P_c(t)$ that a collision occur at time t, $P_c(t) \equiv P(t)\times dt/\tau_c$ since this is the probability that a particle survives for time t and then undergoes a collision. The variance of the collision time is obtained similarly,

$$\langle t^2\rangle=\int_0^\infty t^2\frac{1}{\tau_c}e^{-t/\tau_c}\,dt=2\tau_c^2 \tag{26}$$

and determines the average squared displacement of the particle between one collision and the next, $\langle x^2\rangle=v^2\langle t^2\rangle=2v^2\tau_c^2$, where v is the r.m.s. velocity at the given temperature, $v^2 \equiv \nu k_BT/m$ if classical equilibrium prevails. Then, upon identifying $l_w^2=\langle x^2\rangle$ and $\Gamma_w=\tau_c^{-1}$, we obtain the diffusion coefficient

$$D=\frac{\langle x^2\rangle}{2\nu\tau_c}=\frac{v^2\tau_c}{\nu} \tag{27}$$

and the Einstein relation

$$D=\frac{k_BT}{m\gamma}=\mu k_BT \tag{28}$$

where $\gamma=\tau_c^{-1}$ is the relaxation rate (damping coefficient) and $\mu=1/m\gamma$ the particle mobility under an external driving field (i.e., the limiting velocity for unit field strength). The latter is a kind of fluctuation–dissipation relation, and could also be obtained more generally by observing that, under the influence of a uniform driving field $\mathbf{F}$ along a direction $-z$ (e.g., gravity), the equilibrium concentration profile $n(z) \propto \exp(-Fz/k_BT)$ is realized when the particle flux $\mathbf{j}=-D\nabla n$ offsets the drift $\mathbf{j}_d=n\mu\mathbf{F}$.

Equation 28 expresses the diffusion coefficient in terms of a single microscopic parameter, the relaxation rate γ or the collision time τ_c, and shows that the free diffusion coefficient depends linearly on the temperature. Despite the simplicity of the arguments used in its derivation, this result is rather general: if the "Markov approximation" fails and the particle keeps some memory after a collision, the damping coefficient becomes frequency dependent [$\gamma \to \tilde{\gamma}(\omega)$, where $\tilde{\gamma}$ comes from the Fourier analysis of the memory] but the motion remains diffusive and only the $\omega = 0$ limiting value of $\tilde{\gamma}(\omega)$ matters for the diffusion coefficient (i.e., in *Eq.* 28 $\gamma \to \tilde{\gamma}(0)$)[40]; if the particles motion is quantum, the short time behavior of $\langle \mathbf{x}^2\rangle_t$ may differ from the classical result, but the long-time limit remains classical,[41] and so is the expression of the diffusion coefficient, *Eq.* 28.

When the thermal energy k_BT is lower than the energy of the diffusion barriers, adsorbates are confined in the energy minima and diffusion proceeds through a hopping mechanism. The energy fluctuations induced by the coupling with the phonon bath (or the inherent quantum fluctuations of the system) determine the possibility of random jumps from one adsorption site to a next one. To derive a simple description, we will assume that hopping is much slower than equilibration, so that between two consecutive jumps there is enough time for thermal equilibrium to set in. In this way, two subsequent jumps are not correlated, or—in other words—the diffusion is a Markov process.

In this hopping regime, we can write the average squared displacement over a surface as a sum over contributions from the attainable sites

$$\langle \mathbf{x}^2\rangle_t=\sum_\xi \Gamma_\xi r_\xi^2 t \tag{29}$$

where Γ_ξ is the hopping rate to the ξth site and r_ξ is its distance from the starting site. Consequently, the overall diffusion coefficient can be

written as $D=\frac{1}{2\nu}\sum_{\xi=1}^{N}\Gamma_\xi r_\xi^2$ where $\nu=2$ for a surface. If the surface is isotropic and the hopping events involve only the symmetry equivalent nearest neighbors, the sum is restricted to N equal terms, each having the same distance r and the same hopping rate Γ_s

$$D=\frac{1}{4}N\Gamma_s r^2=\frac{1}{4}\Gamma_e r^2 \tag{30}$$

where $N\Gamma_s=\Gamma_e$ is the total escape rate from the starting adsorption site. In the last formula, all the dynamical information is condensed in Γ_s (or Γ_e) while the rest of the parameters are defined by the arrangement of the surface. In fact when diffusion proceeds mainly by nearest-neighbors jumps, both N and r are fully determined by the symmetry of the surface (Figure 5). For instance, for an atom adsorbing on the top sites of a FCC (111) surface, $N=6$ and r is equal to the lattice constant a; the diffusion coefficient is hence given by $D=\frac{\Gamma_e}{4}a^2=\frac{3}{2}\Gamma_s a^2$. Similarly, for adsorption on the top site of a (100) surface $N=4$ and $D=\Gamma_s a^2$. When the adsorbate binds to the hollow site of a (100) surface, the number of attainable sites and the average hopping distance are unaltered. Instead, for the (111) surface, $N=3$ and $r=\frac{a}{\sqrt{3}}a$ so that $D=\frac{1}{12}\Gamma_e a^2=\frac{1}{4}\Gamma_s a^2$.

More generally, if the surface is not symmetric and non-equivalent sites are accessible, diffusion becomes anisotropic and individual hopping rates are needed. In this case, the particle flux is no longer parallel to the concentration gradient and the scalar diffusion coefficient D needs to be replaced by a 2×2 tensor (in 2D). The tensor is symmetric (both D_{xy} and D_{yx} accompany $\partial^2 f/\partial x\partial y$ in the corresponding diffusion equation) and can thus be put in diagonal form by an appropriate rotation of the coordinate system: along its principal directions $i=X,Y$ one has distinct diffusion coefficients

$$D_i=\frac{1}{2}\sum_\xi \Gamma_\xi(\mathbf{r}_\xi)_i^2$$

where $(r_\xi)_i=\mathbf{r}_\xi\mathbf{e}_i$ is the projection onto the ith principal axis of the position vector of the ξth site; the averaged trace $D=\sum_{i=1}^{\nu}D_i/\nu$, then, describes overall diffusion, but it is meaningful only if the surface is symmetric enough or if it is made up of randomly oriented crystallites.

The rate Γ_s is dictated by the dynamics of the hopping event. When the force driving transport is thermal excitation, it can be determined using Transition State Theory (TST), which assumes that a pseudo-equilibrium is established between the starting condition—the particle at the bottom of the adsorption well—and the transition state located at the top of the diffusion barrier E_d. In our problem, the use of this approach is only justified if jumps are limited to nearest neighbor sites. Furthermore, transition state theory is known to work only for thermal energies smaller than E_d, where TST provides a reliable upper bound to the exact (classical) rate; higher energies lead to re-crossing and cause the diffusing particle to get back to the starting minimum, thereby making the TST upper bound useless[§]. With this premise in mind, the (classical) transition rate expression for Γ_s reads as

$$\Gamma_s=\frac{k_BT}{h}\frac{z^\ddagger}{z}e^{-\beta E_d}=\frac{k_BT}{h}\exp\left(\frac{\Delta S^\ddagger}{k_B}\right)e^{-\beta E_d} \tag{31}$$

where z is the adsorbate partition function referenced to the bottom of the adsorption well, $z^\ddagger$ is a TS partition function referenced to the barrier top, $\Delta S^\ddagger$ is the entropy change between the initial and the transition state, E_d is the diffusion barrier and $\beta=1/k_BT$, as usual. In the simple case of one dimensional hopping of a structureless adsorbate uncoupled to the phonon bath, $z^{-1}\approx\beta\hbar\omega_0$ and the expression above simplifies to

$$\Gamma_s\approx\frac{\omega_0}{2\pi}e^{-\beta E_m} \tag{32}$$

Where ω_0 is the frequency of the adsorbate vibration which leads to barrier crossing, the so-called "attempting frequency", $\omega_0\sim10^{14}$ s^{-1} in typical situations.

In his celebrated work, Kramers[42,43] investigated classical barrier crossing under the influence of a friction γ and obtained some expressions which generalize *Eq.* 32 in the presence of a coupling to the phonon bath. In the moderate-to-strong friction regime, $\gamma/\omega_d>k_BT/E_d$ where ω_d is the frequency of the inverted potential at the barrier top, the Kramers' rate reads as

$$\Gamma_s=\frac{\sqrt{\frac{1}{4}\gamma^2+\omega_d^2}-\frac{1}{2}\gamma}{\omega_d}\frac{\omega_0}{2\pi}e^{-\beta E_d} \tag{33}$$

This is the so-called spatial-diffusion-limited rate which becomes vanishingly small for increasing friction, i.e. (Smoluchowski limit)

$$\gamma/\omega_d\gg k_BT/E_d\ \ \Gamma_s\approx\frac{\omega_0\omega_b}{2\pi\gamma}e^{-\beta E_d}$$

Equation 33 was later re-obtained (and generalized to memory friction) by applying transition-state-theory to the multidimensional problem involving the diffusing particle and the phonon bath.[43–45] The improved rate, *Eq.* 33, is smaller than Γ_s given by *Eq.* 32, a simple manifestation of the variational character of TST. The simple one-dimensional TST result of *Eq.* 32 is recovered only for $\gamma=0$ where, however, TST is completely inadequate (i.e., it provides an unreliably large upper bound to the true rate). Indeed, in the case of weak friction, $\gamma/\omega_d<k_BT/E_d$, particle escape becomes diffusion in energy space and the hopping rate is given by

$$\Gamma_s=\frac{\gamma}{k_BT}\frac{E_d}{\omega_d}\frac{\omega_0}{2\pi}e^{-\beta E_d} \tag{34}$$

We thus see that the hopping rate decreases for both $\gamma\to0$ and $\gamma\to\infty$, and attains its maximum at intermediate values of γ. This is a simple manifestation of the twofold influence of the environment. On the one hand, in the strong friction regime, the increase of γ results in a stronger energy dissipation, which considerably slows down the process of barrier crossing. On the other hand, in the weak friction regime, increasing γ increases the strength of fluctuations (which is proportional to γ), thereby helping the system to cross the barrier.

The above results hold for thermal energies not too smaller than E_d. At very low temperatures thermal fluctuations become negligible, and hopping is primarily determined by tunneling of the system through the diffusion barrier. In this case, the rate can be written as

[§] If $k_BT\gg E_d$ there is no separation of time-scales between barrier crossing and aging, and a kinetic description of the hopping process is impossible. This is the free-diffusion limit discussed above.

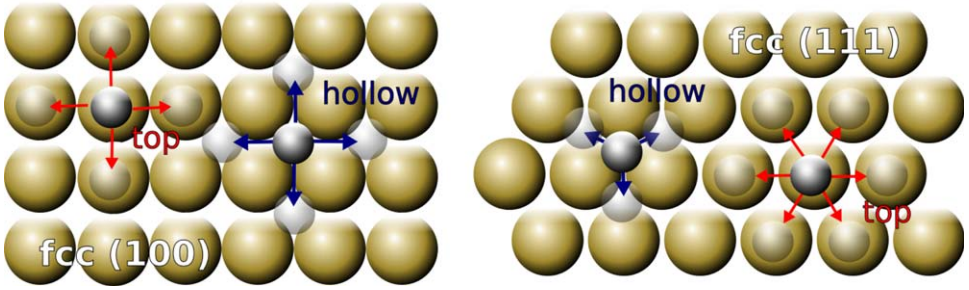

FIGURE 5 Some typical surface structures, adsorption sites and jumps

$$\Gamma_s = \sum_v p_v(T)\Gamma_v^t \tag{35}$$

where $p_v(T)$ is the thermal occupation probability of the vth quantum level of the adsorption well and Γ_v^t is the tunneling rate from that level. In this case a rather different (very weak) dependence on T is expected, and Γ_s approaches a limiting value for $T \to 0$ which is provided by the tunneling escape rate from the ground-state in the adsorption well. Notice, though, that the lattice does play a role in this limit too, even if the coupling is too small to affect the tunneling rate: it determines the loss of coherence in adatoms dynamics, without which the dynamics would be governed by a "band structure," as it is appropriate for a quantum particle on a periodic potential.

5 | VIBRATIONAL RELAXATION

Vibrational relaxation plays an important role in the dynamics at surfaces, and governs the establishment of the equilibration conditions. The time scale of vibrational relaxation determines whether or not a dynamical event comes close to an end, and a stepwise (kinetic) description is appropriate for the overall process or some more complex dynamical pathways need to be considered. So far we have implicitly assumed that it occurs somehow and just exploited its consequences. In the previous sections, for instance, we have seen how a gas-phase species may be trapped onto the surface, and assumed that relaxation was so much faster than desorption that any trapped species was eventually converted into a stuck species. Even the simple analysis of the mechanical energy transfer that occurs when a projectile hits the surface made use of the fact that relaxation of the surface atom(s) hit by the projectile is faster than any competing process, and this allowed us to use kinematics to obtain simple expressions for the amount of energy left on the surface.

Now we look a bit into the details of such process, considering a "vibrator" (being it an ad-species on the surface or an excited surface atom) and its dynamics under the influence of the lattice. Under typical conditions, the thermal energy is much smaller than the vibrational quantum and this makes a quantum treatment necessary. The interest is then in the rate of transition $\gamma_{v_f v_i}$ from a given vibrational state v_i to a given final state v_f, which can eventually be used in a master equation to investigate population and energy decay. In the following we focus on the weak coupling regime and use the Fermi's golden rule to write down explicit expressions for the vibrational relaxation rates; the same results follow from the general linear response theory when applied to compute (up to second order) the change in the density operator induced by the vibration–phonon interaction.

We consider the following model Hamiltonian

$$H = \frac{p_z^2}{2m} + v(z) + \sum_k \left(\frac{p_k^2}{2m_k} + \frac{m_k \omega_k^2 q_k^2}{2} \right) + H_{\text{int}} = H_0 + H_{\text{int}}$$

where a vibrational degree of freedom z is coupled to a phonon bath of coordinates q_k; the potential $v(z)$ and the interaction term H_{int} may take a general form. We are interested in the rate of transition between stationary states $I = (v_i, \mathbf{i})$ and $F = (v_f, \mathbf{f})$ of the uncoupled Hamiltonian H_0, where v_i, v_f label states of the vibrator and $\mathbf{i} = (i_1, i_2, ..i_k, ..)$ and $\mathbf{f} = (f_1, f_2, ..f_k, ..)$ are bath states with $i_1(f_1)$ phonons in Mode 1, $i_2(f_2)$ phonons in Mode 2, $i_k(f_k)$ phonons in Mode k, etc. The corresponding energies are $E_I = \varepsilon_{v_i} + E_{\mathbf{i}}$ and $E_F = \varepsilon_{v_f} + E_{\mathbf{f}}$, where $\varepsilon_{v_i}(\varepsilon_{v_f})$ are vibrator energies and $E_{\mathbf{i}} = \sum_k \hbar\omega_k (i_k + \frac{1}{2})$ $(E_{\mathbf{f}} = \sum_k \hbar\omega_k (f_k + \frac{1}{2}))$ are bath energies. The Fermi's golden rule expression for the microscopic transition rate reads as

$$\Gamma_{F \leftarrow I} = \frac{2\pi}{\hbar} |\langle F|H_{\text{int}}|I\rangle|^2 \delta(E_F - E_I)$$

and, in general, allows transitions between arbitrary phonon states. However, if the coupling is close to be linear in bath coordinates,

$$H_{\text{int}} \approx \sum_k V_k q_k = \sum_k V_k \Delta q_k (a_k + a_k^\dagger)$$

only transitions between states that differ by one phonon are allowed

$$\langle F|H_{\text{int}}|I\rangle = \begin{cases} \sqrt{i_k}\Delta q_k \langle v_f|V_k|v_i\rangle & \text{if} \quad \mathbf{f} = \mathbf{i} - \mathbf{1}_k \\ \sqrt{i_k + 1}\Delta q_k \langle v_f|V_k|v_i\rangle & \text{if} \quad \mathbf{f} = \mathbf{i} + \mathbf{1}_k \\ 0 & \text{otherwise} \end{cases}$$

where $\mathbf{1}_k$ is the kth canonical vector, i.e. with a 1 in the kth position and zero otherwise. Hence, upon averaging over the bath initial states and summing over the final states we can write the vibrational transition rate in the form

$$\gamma_{v_f v_i} = \frac{2}{\hbar} I(|\omega_{v_f v_i}|) \begin{cases} n_\beta(|\omega_{v_f v_i}|) & \omega_{v_f v_i} > 0 \\ n_\beta(|\omega_{v_f v_i}|) + 1 & \omega_{v_f v_i} < 0 \end{cases}$$

where $\omega_{v_f v_i} = (\varepsilon_{v_f} - \varepsilon_{v_i})/\hbar$ is the Bohr frequency, $n_\beta(\omega) = (e^{\beta\hbar\omega} - 1)^{-1}$ the Bose–Einstein occupation function and

$$I_{v_f v_i}(\omega) = \frac{\pi}{2} \sum_k \frac{|\langle v_f|V_k|v_i\rangle|^2}{m_k \omega_k} \delta(\omega - \omega_k)$$

is the appropriate spectral density of the coupling that subsumes both the strength of the vibration–phonon interaction and the density of phonon modes. In the above expression $\omega_{v_f v_i}>0$ refers to upward transitions (↑) and $\omega_{v_f v_i}<0$ refers to downward transitions (↓), similar to photon absorption and photon emission processes. The first can only be phonon-induced and occurs with a rate proportional to the number of phonons at the required frequency; the latter, on the other hand, have a spontaneous contribution $\eta_{v_f v_i}=2I(\omega_{v_f v_i})/\hbar$ which adds to the phonon-induced one. Clearly, under the above circumstances, only the rate of the spontaneous emission $\max\{v_f, v_i\} \rightarrow \min\{v_f, v_i\}$ is needed, the others are easily obtained from known thermal factors, namely $\gamma_{fi}^{\uparrow}=\eta_{if}\times n(\omega_{fi})$ and $\gamma_{fi}^{\downarrow}=\eta_{fi}\times(n(\omega_{if})+1)$. At equilibrium, detailed balance holds, i.e. $\gamma_{fi}p_i=\gamma_{if}p_f$ (p_i being the probability that the system is found in state i), and we obtain the equilibrium distribution of the vibrator $p_f=p_i e^{-\beta\hbar\omega_{fi}}$.

Of particular interest is the case where H_{int} is further linear in z, since it allows one to extract general trends. In that case, in fact, $V_k=c_k z$ and $I_{v_f v_i}(\omega)=|\langle v_f|z|v_i\rangle|^2 J(\omega)$ where

$$J(\omega)=\frac{\pi}{2}\sum_k \frac{c_k^2}{m_k\omega_k}\delta(\omega-\omega_k)$$

completely characterizes the coupling to the phonon bath. If the vibrator is well approximated by a harmonic oscillator of frequency ω_0, only $\Delta v=\pm 1$ transitions are allowed,

$$\langle v_f|z|v_i\rangle=\sqrt{\frac{\hbar}{2m\omega_0}}\left(\sqrt{v_i}\delta_{v_f,v_i-1}+\sqrt{v_i+1}\delta_{v_f,v_i+1}\right)$$

and the downward rates depend linearly on v_i (on v_i+1 for the upward rates). They can be obtained from the rate of the $0 \leftarrow 1$ spontaneous emission $\eta_{0,1}=J(\omega_0)/m\omega_0$,

$$\eta_{v,v+1}=v\,\eta_{0,1}$$

and this provides a very useful scaling rule.

Realistic systems are neither linear in the bath coordinates nor in the system one. Thus, the apparent similarity with photon absorption/emission problems does not hold in practice, and multiphonon absorption/emission processes are the rule rather than the exception. To see the new physics emerging in such problems, we consider an interaction of the product form, $H_{int}=f\times\Phi$ where $f(\Phi)$ is a system (bath) operator, and assume that thermal equilibrium conditions prevail for the phonon bath.[46] This allows us to re-write the Fermi's golden rule rate in an alternative form, that is very useful in practice. To this end, we replace the energy-conserving δ-function with its Fourier representation and perform the appropriate sums over bath states. We find

$$\gamma_{v_f v_i}=\sum_{f,i} p_i\Gamma_{F\leftarrow I}\equiv\frac{|f_{v_f v_i}|^2}{\hbar^2}\int_{-\infty}^{+\infty} dt e^{i\omega_{v_f v_i}t}\langle\Phi(0)\Phi(t)\rangle_\beta \qquad (36)$$

where $f_{v_f v_i}=\langle v_f|f|v_i\rangle$, and

$$\langle\Phi(0)\Phi(t)\rangle_\beta=\mathrm{Tr}_B\left(\rho_\beta\Phi(0)\Phi(t)\right)$$

is a canonical autocorrelation function of the operator Φ at a temperature $T=1/k_B\beta$. In the last expression, ρ_β is the equilibrium density operator of the phonon bath, and $\Phi(t)$ is the Heisenberg-picture Φ operator, $\Phi(t)=e^{iH_B t/\hbar}\Phi e^{-iH_B t/\hbar}$, H_B being the phonon bath Hamiltonian.

Next, we take Φ of the exponential form

$$\Phi=\exp(\alpha q_S)=\exp\left(\alpha\sum_k u_k q_k\right)$$

where α^{-1} is a characteristic length of the interaction and q_S is a collective coordinate (a combination of phonon modes), and compute the required correlation function. With the help of the Baker–Haussdorf identity, *Eq.* 10, we write the product of operators that appears in the correlation function by gathering all operators in a single exponential

$$\begin{aligned}\Phi(0)\Phi(t)&=\exp(\alpha q_S(0))\exp(\alpha q_S(t))\\&=\exp(\alpha[q_S(0)+q_S(t)])\exp\left(\frac{\alpha^2}{2}[q_S(0),q_S(t)]\right)\end{aligned}$$

where $q_k(t)=\Delta q_k(a_k e^{-i\omega_k t}+a_k^\dagger e^{+i\omega_k t})$, $q_S(t)=\sum_k u_k q_k(t)$ and $[q_S(0), q_S(t)]$ is a c-number ($[q_S(0),q_S(t)]\equiv 2i\sum_k \Delta q_k^2 u_k^2\sin(\omega_k t)$). Finally, we use the Bloch identity

$$\langle\exp(L)\rangle_\beta=\exp\left(\frac{\langle L^2\rangle_\beta}{2}\right)$$

to evaluate the correlation function. This identity holds for arbitrary linear combinations L of the coordinates and momenta operators in general, linear systems in canonical equilibrium, and follows from the fact that, under such circumstances, L is zero-centered Gaussian distributed,[41] i.e.

$$\langle L^{2n+1}\rangle_\beta=0\quad\langle L^{2n}\rangle_\beta=\frac{(2n)!}{n!}\left(\frac{\langle L^2\rangle_\beta}{2}\right)^n$$

The final result is

$$\langle\Phi(0)\Phi(t)\rangle_\beta=e^{\alpha^2\langle q_S^2\rangle_\beta}e^{\alpha^2\langle q_S(0)q_S(t)\rangle_\beta} \qquad (37)$$

where

$$\langle q_S(0)q_S(t)\rangle_\beta=\frac{\hbar}{\pi}\int_0^\infty J(\omega)\left[\coth\left(\frac{\beta\hbar\omega}{2}\right)\cos(\omega t)+i\sin(\omega t)\right]d\omega$$

is the position correlation function of the collective mode, $\langle q_S^2\rangle_\beta \equiv \langle q_S(0)q_S(0)\rangle_\beta$ the squared width of its equilibrium distribution and

$$J(\omega)=\frac{\pi}{2}\sum_k\frac{u_k^2}{m_k\omega_k}\delta(\omega-\omega_k)$$

is the appropriate spectral density of the coupling. The rate then reads as

$$\gamma_{v_f v_i}=\frac{|f_{v_f v_i}|^2}{\hbar^2}e^{\alpha^2\langle q_S^2\rangle_\beta}\int_{-\infty}^{+\infty}dt\,e^{i\omega_{v_f v_i}t}\exp\left(\alpha^2\langle q_S(0)q_S(t)\rangle_\beta\right) \qquad (38)$$

and contains multiphonon transitions already at the adopted theory level (first order in perturbation theory): the correlation is linear in the phonon occupation function and appears in the exponent.

An exponential coupling model arises for instance when the vibrator couples strongly to a surface atom q_S through an anharmonic (Morse) surface potential,

$$H_{int}(z,q_S)=V(z-q_S)=De^{-\alpha(z-q_S)}\left(e^{-\alpha(z-q_S)}-1\right)\approx -2\alpha D\Phi(q_S)z \text{ for } z\approx 0$$

with

$$\Phi(q_S)=e^{\alpha q_S}(e^{\alpha q_S}-1)$$

For this specific interaction term we obtain, after some algebra,

$$\langle \Phi(0)\Phi(t)\rangle_\beta = e^{4\alpha^2\langle q_S^2\rangle_\beta} e^{4\alpha^2\langle q_S(0)q_S(t)\rangle_\beta} + e^{\alpha^2\langle q_S^2\rangle_\beta} e^{\alpha^2\langle q_S(0)q_S(t)\rangle_\beta} - 2e^{\frac{5}{2}\alpha\langle q_S^2\rangle_\beta} e^{2\alpha^2\langle q_S(0)q_S(t)\rangle_\beta}$$

Differently from *Eq*. 37 this expression has the correct limiting behavior

$$\alpha \to 0 \quad \langle \Phi(0)\Phi(t)\rangle_\beta \to \alpha^2\langle q_S(0)q_S(t)\rangle_\beta$$

in the weak coupling limit, as it follows from the judicious choice of the interaction term which becomes bilinear in vibration-phonon coordinates ($H_{int} \to -2\alpha^2 D z q_S$ in the above limit). The corresponding rate follows from *Eq*. 36 and generalizes *Eq*. 38 to realistic gas-surface systems; similar results can be obtained, more generally, when the popular independent oscillator model (see Appendix) is extended to nonlinear phonon baths[47] in the context of the effective mode theory.[48–51]

6 | DESORPTION

At high temperature diffusion is limited by the competition with desorption, the process in which a trapped particle overcomes the adsorption barrier and returns to the gas phase. Similarly to diffusion, we can estimate the probability of desorption by applying TST to a one dimensional reaction coordinate that goes from the adsorption well to the top of the barrier. In this description, the desorption probability is given by

$$P_{des} \approx \frac{\omega_0}{2\pi} e^{-\beta E_{des}} \tag{39}$$

where E_{des} is the desorption barrier energy, i.e. the adsorption energy plus the adsorption barrier (if any), and ω_0 is the frequency of the "surface stretching," i.e. the vibrational mode that elongates the bond between the surface and the adsorbate. Also in the case of desorption, the effect of the coupling to the surface can be incorporated with Kramers theory, and a damping dependent pre-factor introduced. The relevant formulas for the weak and strong friction regimes have already been given in Eqs. 33 and 34, and need no further comments.

One of the reasons for the interest in the desorption lies in the possibility to use it to gain information on the inverse process, namely adsorption. The time-reversal symmetry of the equations of motion (for the adsorbate and the surface in conjunction) implies the validity of the principle of detailed balance, which relates the probabilities for the two events. Let $P_s(\varepsilon, n, T)$ be the probability that a particle in a specific internal state n with a given incidence energy ε is adsorbed on a surface at temperature T. Further let $P_d(\varepsilon, n, T)$ be the probability that a particle adsorbed on a surface at temperature T desorbs and emerges to the gas-phase with a kinetic energy ε in an internal state n. The principle of detailed balance requires that P_s and P_d are related by

$$P_d(\varepsilon, n, T) \propto P_s(\varepsilon, n, T) \exp\left(-\frac{E_n + \varepsilon}{k_B T}\right) \tag{40}$$

with E_n being the energy associated to the internal state of the particle.

7 | REACTIONS

We now turn the attention to some elementary reactions, some processes in which either a new bond is formed (the Eley–Rideal, Langmuir–Hinshelwood, and Hot-Atom molecule formation) or an existing bond is broken (the Dissociative Chemisorption of a molecule) because of the presence of a surface. In all these processes, besides its possible key catalytic effect on the kinetics, the surface plays a simple but unique role: it may act as a sink that dissipates the reaction energy, thereby allowing reactions that would be otherwise forbidden. This is clear when considering the general "recombination reaction" between two species A and B to give the product AB: without a "third body" that takes the excess of energy away from the colliding partners such a process *cannot* occur, and is thus extremely slow in low density environments where only the photon bath—the ubiquitous electromagnetic field—is available for exchanging energy. This was the case of the interstellar medium prior to the first generation of stars (the so-called Early Universe) that underwent a kind of "chemical revolution" when the first surfaces (those of the dust grains freed by stellar explosions) appeared.

The presence of a relatively large number of degrees of freedom often makes hard to derive a comprehensive, yet simple analytical treatment of the processes under consideration. Thus, in the following, we shall only focus on those aspects that can be interpreted in terms of simple mechanical concepts, and use them to extract general trends.

7.1 | Eley–Rideal

The Eley–Rideal mechanism is one of the possible routes for the formation of a molecular species mediated by the presence of a surface. It is a direct dynamical process, in which an atom or a molecule from the gas phase (the incidon) collides with another species (the targon), initially adsorbed on and in thermal equilibrium with the surface. As a consequence, under carefully controlled conditions, product molecules show some signatures of the pre-collisional state, e.g. a dependence on the incidence angle.[52–56] Among the surface recombination processes, this is the most exothermic one: only a single surface-atom bond gets broken and this is generally weaker than that holding the atoms together in the product molecule. Since only a fraction of the excess energy is deposited on the surface, the reaction exoergicity generally produces rovibrationally hot and fast moving molecules, the exact energy partitioning depending on the details of the molecular formation process.

Generally speaking, the Eley–Rideal dynamics (and the size of the corresponding reaction cross-section) largely depends on the strength of the atom-surface bond(s).[57] When the target is strongly bound to the surface—as it happens for hydrogen atoms on metal surfaces where the binding energy is ~2.5 eV—it is also placed very next to it. Under such circumstances, for the reaction to occur the projectile needs to get near the surface, and only in close encounters it can tear the target off the surface attraction. In addition, if the projectile-surface bond is comparably large (e.g., when H recombines with H on a metal surface), incoming trajectories are focused along the surface normal, and hardly adjust their in-plane position before bouncing off the

surface. As a consequence, in this case, reaction cross-sections are small, $\lesssim 1$ Å^2, and only weakly dependent on the collision energy: only small impact parameter trajectories successfully end up in reaction, and the surface-atom interaction energy dominates over the collision energy. On the other hand, when the target-surface bond is weak-to-moderate the target is placed well above the surface and better "exposed" to the projectile, which thus does not need to come close to the surface to form the reaction product. In this case, the effect of the projectile-surface interaction is less drastic, and large impact parameter trajectories may find their way to react, too. As a result, Eley–Rideal cross-sections become large and with a marked dependence on the collision energy which signals a competition between different attractive interactions (projectile-target vs. projectile-surface).

Hence, we see that two different collision mechanisms are potentially operative. Small impact parameter trajectories undergo head-on collisions, give only a small contribution to the reaction cross-section and lead to the vibrationally hottest product molecules, at the expense of a negligible rotational excitation. Large impact parameter trajectories, if possible, undergo glancing collisions, give a major contribution to the reaction cross-section and allow rotational excitation of the products.

In head-on collisions the reaction is governed by the energy transfer from the projectile to the target. Hence, the dependence of the reaction probability on the collision energy of the projectile species is well captured by a simple, impulsive model of the dynamics, analogous to that introduced above for the sticking dynamics.[58] In this model, the projectile with mass m_P and speed $v_P=\sqrt{2\varepsilon/m_P}$ undergoes a binary collision with the target of mass m_T and speed v_T, slows down its motion, and gets captured by the targon after the latter elastically bounces off the surface. Reaction occurs when the final kinetic energy of the targon ε'_T is larger than ε^*, a dynamical threshold that we introduce to replace the details of the dynamics and filter out those trajectories in which the target is too slow to capture the projectile before leaving the reaction region. Also in this case, conservation of mechanical energy and of linear momentum translate into some simple kinematic conditions. Unlike the sticking dynamics, though, the main acceleration might be provided by the target-projectile interaction, and be in the relative velocity v rather than in laboratory velocity v_T. This is the case, for instance, of formation of H_2 isotopologues on graphite, where the H–H attraction dominates over the H–surface interactions. The exit targon velocity v'_T, given by

$$v_T^{'}=-V-\frac{\mu}{m_T}\tilde{v} \tag{41}$$

results from the acceleration of the colliding pair, the projectile-target collision and the bounce of the targon off the surface. Here V is the center of mass speed of the colliding pair, $\tilde{v}^2=v^2+2D_m/\mu$ (D_m being the projectile-targon well depth) and μ the reduced mass of the binary system. The final kinetic energy of the targon is subjected to a reaction condition, namely $\varepsilon'_T(v_T,v_P)>\varepsilon^*$, which determines a domain $\mathcal{I}(\varepsilon)$ of target velocities leading to reaction ($\mathcal{I}(\varepsilon)$ depends on the collision energy $\varepsilon=m_Pv_P^2/2$). Finally, the Eley–Rideal reaction probability $P_{ER}(\varepsilon)$ is obtained by integrating the distribution of target velocities $g(v)$ over $\mathcal{I}(\varepsilon)$. In the simplest case, $g(v)$ is simply related to the momentum space wavefunction ($\phi_v(p)$) of the target initial vibrational state—i.e. through $g(v)=m_T|\phi_v(m_Tv)|^2$—but a corrective factor has to be expected on general grounds to account for the fact that the collision is hardly in the true impulsive limit ($\tau_c\omega_0 \ll 1$, τ_c being the collision time and ω_0 the targon vibrational frequency).

On the other hand, glancing collisions, which become relevant when the targon–incidon potential dominates the dynamics, occur for large impact parameters and are ruled by the *orbital* angular motion of the colliding pair. In this case it is more appropriate to think about the reaction as a "capture" of the projectile by the target. If it were for the binary system interaction only, knowledge of the long-range tail of the projectile-targon potential would suffice to determine the "capture radius" ρ_c at a given energy ε, *i.e.* the maximum value of the impact parameter for which capture does occur (and then the size of the capture cross-section $\sigma=\pi\rho_c^2$). For a potential of the form $U(r)\approx -\alpha/r^n$ ($n>2$), one readily obtains

$$\rho_c=\sqrt{\frac{n}{n-2}}\sqrt[n]{\frac{n}{2}-1}\sqrt[n]{\frac{\alpha}{\varepsilon}} \tag{42}$$

This result holds for collisions in the gas-phase and determines, for instance, the Langevin capture rate that accurately describes low-temperature ion-molecule reactions ($n=4$) (the assumption here is that once the ion–molecule complex is formed, reaction occurs with unit probability).[59] In our gas-surface case, however, the projectile–targon attraction competes with the projectile–surface interaction and this competition strongly modifies the energy dependence of ρ_c. The surface is seen to *shield* the targon from low-energy projectiles and, conversely, to *focus* higher energy trajectories toward the target, thereby reducing (increasing) the capture radius at low (high) collision energies.

This is best seen in a simple model where the targon is held fixed at a height h ($h>0$ when the target atom lies above the "surface") and the surface is represented by a hard wall that has the simple effect of reverting the normal component of the projectile velocity, $v_z \to -v_z$ (see Figure 6). In this model, the relative orbital angular momentum of the projectile target binary system undergoes a sudden change $l \to l'$ upon collision with the surface, namely

$$\Delta l^2=l'^2-l^2=-4uhv_xv_z \tag{43}$$

if $\mathbf{r}_P=(u,-h)$ represents the projectile position in the scattering plane (referenced to the targon) at the time of the impact and $\mathbf{v}=(v_x,v_z)$ its speed (Figure 6). Since for an attractive interaction $v_xv_z \geq 0$ (≤ 0) holds to the right (left) of the targon atom, the change Δl is *negative* for a targon above the surface and *positive* otherwise. As a consequence, the effective barrier ruling the capture process decreases (increases) when the target lies above (below) the surface and, correspondingly, the capture radius becomes larger (smaller) than its gas-phase value. Real surfaces are not hard walls and display a more intricate competition with the targon field of forces than the one outlined here. Nevertheless, for the large-impact parameter trajectories we are interested in, the picture above is modified only to the extent that the height of the turning point becomes energy dependent, the smaller the collision energy is the higher the "altitude" where the projectiles reverts its motion.

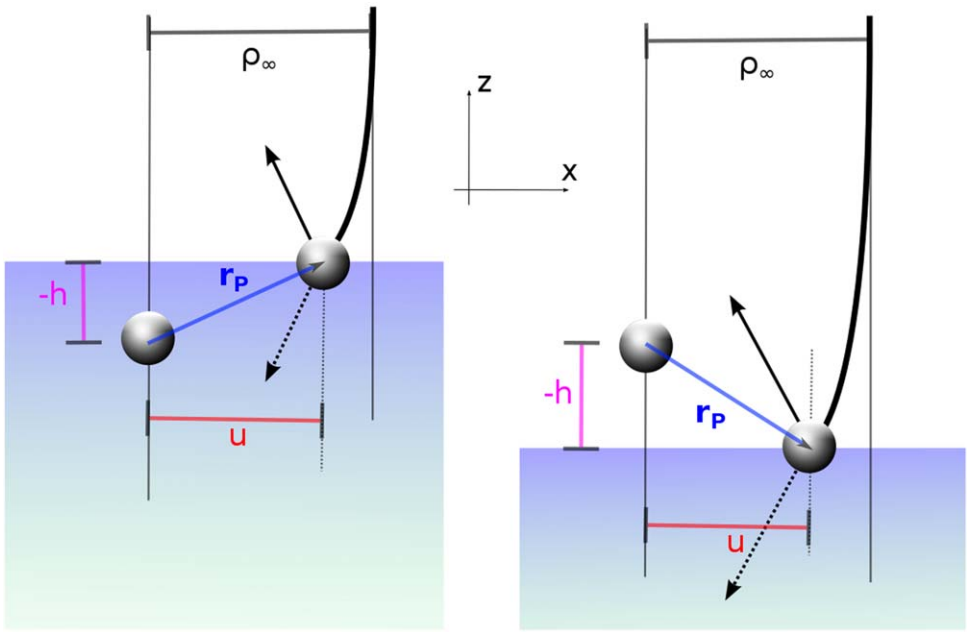

FIGURE 6 A schematics of the hard-wall model used in the main text to illustrate the effect of the surface on projectile capture. The targon is held fixed at a height h above the surface ($h<0$ in the left panel and $h>0$ on the right) and collision of the projectile with the surface occurs at a position $\mathbf{r}_P=(u,h)$ in the scattering plane. The arrows indicate the projectile speed before (dashed) and after (thin line) the bounce and ρ_∞ is the impact parameter of the trajectory

7.2 | Langmuir–Hinshelwood

At ambient conditions, Langmuir–Hishelwood is the most common mechanism for recombination at a gas–solid interface. The elementary microscopic event is particularly simple: two species A and B diffusing on the surface meet and react, forming a product AB that then may leave the surface for the gas phase. Since in the Langmuir–Hinshelwood mechanism diffusion plays a primary role, and eventually impedes reaction at low enough surface temperatures, here we limit ourselves to some simple considerations on the microscopic LH rate constant. The latter takes a slightly different form depending on whether association is thermally activated or proceeds as soon as the reaction partners come close to each other (here, with the term association we mean reaction from two ad-species located in neighboring sites).

We consider a surface at low coverage of atoms and look first at the case in which association is facile. Under these conditions, the time between collisions is much larger than the time involved in a collision and the number of "three-body" encounters is negligible compared to two-body events. We further simplify association and assume that those atoms that come close to each other within a distance σ do react and leave the surface. In this simplified picture, this critical distance σ—the "linear" cross-section of the reaction—does not depend on the velocity of the particles and needs to be of the order of the lattice constant of the surface. Using standard results in the kinetic theory of gases (in two dimensions) we can then write the rate constant as

$$k=v\,\sigma \tag{44}$$

where v is relative velocity of the colliding partners, i.e.

$$v=\sqrt{\langle(\mathbf{v}_A-\mathbf{v}_B)\rangle^2}=\sqrt{v_A^2+v_B^2}$$

if it is taken to be the root-mean-squared one. The appropriate velocities are those describing diffusion of the two species on the surface, and are the thermal velocities when diffusion is free and

$$v_X^2=\frac{4D_X\Gamma_e^X}{N^2}=\frac{16D_X^2}{N^2r_X^2}\quad X=\mathrm{A,B}$$

when diffusion is a thermal hopping process (here D_X is the diffusion coefficient of the species X, Γ_e^X its total escape rate, N the number of hopping sites and r_X the jump length, see *Eq.* 30).

On the other hand, when a barrier E_a is present in AB formation, association is a slow process and can be modeled as a distinct kinetic step. In this case, the rate given above becomes that for having the two partners in neighboring sites (we call AB^* this configuration), and must be corrected to include the association step. The latter occurs with a rate k_a that can be estimated with the help of transition state theory,

$$k_a=\frac{k_bT}{h}\frac{z_{AB}^{\ddagger}}{z_Az_B}e^{-\beta E_a}$$

where z_A is the partition function of reactant A, z_B similarly for B, and $z_{AB}^{\ddagger}$ is the partition function of the transition state. When A and B are simple atoms z_A, z_B take a simple form (e.g., $\sim(k_BT)^3/\omega_{\parallel}^2\omega_{\perp}$ for an adatom placed in a symmetric site with two degenerate in-plane frequencies $\omega_{\parallel}$ and a frequency $\omega_{\perp}$ for the motion along the surface normal) and z_{AB} is only slightly more complicated, being that of an adsorbed diatomic with a hindered translation-like mode. Then, it follows

$$k_{\mathrm{LH}}=k\,\frac{k_a}{k_a+k_d} \tag{45}$$

where $k_d=f_A\Gamma_e^A+f_B\Gamma_e^B$ is the "dissociation" rate of AB^*, given in terms of the total escape rates Γ_e and the fraction $f_X=(N_X-1)/N_X$ of sites

available for "dissociation" ($X=A,B$). *Equation* 45 of course reduces to the previous estimate $k_{LH} \approx k$ when association is a fast process ($k_a \gg k_d$).

7.3 | Hot Atoms

When a light atom impinges on a metal surface, because of the unfavorable mass ratio, it hardly dissipates enough energy to get trapped at the impact site in a single collision (see Eqs. 5 and 6). Nevertheless, there exists the possibility that the intrinsic corrugation of the surface (or that created by any species adsorbed on it) allows some energy to be channeled in the motion *parallel* to the surface, thereby forming trapped but fast moving species. In this case, the light atoms travel along the surface and repeatedly collide with it, eventually transferring enough energy to become permanently trapped. The resulting hot-atoms have energies much in excess to the thermal energy and may react with adsorbed species located tens Å away from the impact position, even when the surface temperature is so small that thermal diffusion cannot occur. Only a small fraction of the initially trapped species finds a collision that re-convert energy in the direction normal to the surface (and thus potentially desorbs before "stabilization" occurs), but also in this case these metastable hot-species may travel for ps along the surface and find a reaction partner prior to desorption.

The situation is common for (but not limited to) H atoms on metal surfaces, where the large value of the binding energy of ~2.5 eV makes trapping easier, and H atoms with ~2 eV kinetic energy along the surface are common. The corresponding reaction mechanism is intermediate between Eley–Rideal and Langmuir–Hinshelwood, and is called Hot-Atom (HA) mechanism.[60] It is not as direct as ER but does proceed neither through thermally equilibrated species like LH. As a result, HA products are typically as hot as Eley–Rideal products, and show limited surface temperature dependence. They are hard to distinguish from ER products in experiments where detailed information on the dynamics cannot be obtained (e.g., kinetic experiments), if not for the extremely large apparent cross-sections they can give rise to.

Modeling of the reaction dynamics proceeds along lines similar to those illustrated above for LH, in the limit where diffusion is free and a linear (most likely energy dependent) cross-section characterizes reactive collisions in two dimensions. The main departure from LH is in the diffusive process: the squared velocity v^2 determining the size of the diffusion coefficient is given by the large, non-equilibrium hot-atom energy rather than its thermal value,

$$D=\frac{v^2\tau_c}{2}=\frac{E_{HA}}{m\gamma}$$

where τ_c (γ) is the collision time (rate), m the hot-atom mass and $E_{HA} \gg k_BT$ its energy. For instance, in a typical situation one finds E_{HA}~2 eV, to be compared with the room-temperature thermal energy of 0.025 eV. Actually, hot-atoms move ballistically for rather long times (ps) that, depending on the surface coverage, the transition from ballistic ($\Delta x^2 \sim t^2$) to diffusive ($\Delta x^2 \sim t$) may not be complete before they react, i.e. in the time window of interest for their dynamics.

We emphasize here that the situation is quite different from that described by the standard Langevin dynamics (see Appendix): hot-atoms do behave essentially free but undergo random *quasi-elastic* collisions changing the direction of their velocity vectors rather than inelastic interactions (collisions) with an equilibrated environment. To better explain this difference, we notice that in the Langevin description of Brownian motion the average energy change "per collision" is a fixed, large fraction of the energy in excess to the thermal one $-\langle\varepsilon\rangle^*=\langle\varepsilon\rangle-\varepsilon_\beta$ where $\langle\varepsilon\rangle=m\langle v^2\rangle/2$ and $\varepsilon_\beta=k_BT/2$ for Brownian motion in 1D—clearly at odds with the energy transfer process of interest here. To see this, let us consider the Langevin equation appropriate for this case

$$m\dot{v}+m\gamma v=\xi$$

(see Appendix, namely *Eq. 56* for $V=0$, and $v=\dot{z}$), multiply it by v and take the ensemble average

$$\frac{d\langle\varepsilon\rangle}{dt}+2\gamma\langle\varepsilon\rangle=\langle v\xi\rangle \tag{46}$$

Here the average $\langle v\xi\rangle$ can be computed from the explicit solution of the LE above, $v(t)=v(0)e^{-\gamma t}+\int_0^t e^{-\gamma(t-\tau)}\xi(\tau)d\tau/m$, and easily seen to be

$$\langle v(t)\xi(t)\rangle=\frac{1}{m}\int_0^t e^{-\gamma(t-\tau)}\langle\xi(\tau)\xi(t)\rangle d\tau=\gamma k_BT$$

where use has been made of the fluctuation-dissipation theorem, *Eq. 57*, for $\gamma(t)=2\gamma\delta(t)$. Thus, energy excess decays exponentially according to $\langle\varepsilon^*\rangle(t)=\varepsilon^*(0)\times\exp(-2\gamma t)$, and the energy transfer per collision is $\delta\varepsilon=|\Delta\langle\varepsilon^*\rangle(\gamma^{-1})| \approx 0.86\langle\varepsilon^*\rangle$ where $\langle\varepsilon^*\rangle$ is the excess energy at the given time. Such collisional energy transfer is small only in near equilibrium conditions (in fact, it is zero in equilibrium because of the fact that energy gain and energy loss processes become equally likely), but it is clearly enormous at the typical hot-atom energies where $\langle\varepsilon^*\rangle \approx \langle\varepsilon\rangle \approx 2$ eV.

Were it not for the slow energy decay, hot atom dynamics could be modeled by free-atom dynamics with a random purely re-orienting force (e.g., a term like $\mathbf{v}\wedge\mathbf{H}$ where $\mathbf{H}$ is a constant, "pseudo-magnetic" field that is randomly switched on parallel or antiparallel to the surface, for variable times t_H), or, more accurately, by simple Hamiltonian dynamics in the fully corrugated static surface potential $V=V_S(\mathbf{x})$. However, introducing energy transfer in a reduced description without resorting to a full lattice dynamics is highly desirable, at least in the "short" time (few ps) where hot atoms stabilize on the surface and slightly slow down their motion before reacting. This is because a full lattice dynamics could be computationally demanding even today, since large simulation cells are required to accommodate hot-atom trajectories. Furthermore, one can also introduce in this way the energy transfer to the electronic system by $e-h$ pair excitations, a process which may occur irrespective of the lattice dynamics.

Fortunately, it turns out that such "quasi-Langevin" description is possible.[61] Energy decay to phonons is a slow process, inelastic collisions are random and memory-less, and roughly limited to the hot-atoms interaction with the repulsive wall of V_S. The resulting stochastic equation of motion for this *rigid*-surface hot-atom dynamics—a Langevin-like equation with state-dependent friction—reads as

$$m\ddot{\mathbf{x}}+\nabla V_S(\mathbf{x})+(\alpha+\zeta)F(\mathbf{x})\frac{\dot{z}}{|\dot{z}|}\hat{\mathbf{z}}=0 \tag{47}$$

where $V_S(\mathbf{x})=V_S^{att}(\mathbf{x})+V_S^{rep}(\mathbf{x})$ is the rigid-surface potential separated in an attractive (att) and a repulsive (rep) contribution and $F(\mathbf{x})=-\partial V_S^{rep}(\mathbf{x})/\partial z \geq 0$ is the repulsive force along the surface normal. Furthermore, $\alpha>0$ is a constant that characterizes energy dissipation (it is the only empirical parameter needed) and ζ is a Gaussian random variable with zero mean that takes a different value each time the hot-atom reverts its motion along the surface normal** (i.e., for $v_z=\dot{z}=0$). The physical interpretation of the above equation is the following. Consider the limiting case where the interaction is separable $V_S(\mathbf{x})=V_{\parallel}(x,y)+V_{\perp}(z)$, i.e., where the motion along z can be treated independently of the motion along the surface plane (x, y). The equation governing energy dissipation is then the 1D equation

$$m\ddot{z}+\frac{d}{dz}\left\{\left[1-(\alpha+\zeta)\frac{\dot{z}}{|\dot{z}|}\right]V^{rep}(z)+V^{att}(z)\right\}=0$$

and describes dynamics on an effective potential

$$V^{eff}(z)=[1\pm(\alpha+\zeta)]V^{rep}(z)+V^{att}(z)$$

where the *plus* sign stands for the atom traveling toward the surface ($v_z<0$) and the *minus* for the opposite case. At each collision there is a jump in the *total* energy, which though is substantial only at the inner turning point, since V^{rep} is negligible at large z. For such $v_z<0 \rightarrow v_z>0$ collision the energy change reads as

$$\delta\varepsilon=-2(\alpha+\zeta)V^{rep}(z_{tp})=-2(\alpha+\zeta)\frac{\varepsilon-V^{att}(z_{tp})}{1+\alpha+\zeta}$$

(where ε is the incidence energy) and corresponds to energy transferred from the hot-atom to the lattice. This means that the average energy change per collision is

$$\langle\delta\varepsilon\rangle \approx -2\alpha\varepsilon$$

(for $\alpha,\zeta \ll 1$ and $\varepsilon \gg V^{att}(z_{tp})$). Similarly, $(\delta\varepsilon)^2 \approx 4(\alpha+\zeta)^2\varepsilon^2$, and the average energy fluctuation per collision turns out to be

$$\langle\Delta(\delta\varepsilon)^2\rangle=\langle(\delta\varepsilon)^2\rangle-\langle\delta\varepsilon\rangle^2=4\langle\zeta^2\rangle\varepsilon^2$$

Comparison with Langevin dynamics determines the size of the fluctuations $\langle\zeta^2\rangle$ in the random term. To this end, we notice that in the Langevin dynamics the energy fluctuations obey the equation

$$\frac{d\langle\Delta\varepsilon^2\rangle}{dt}=2\left[-2\gamma\langle\Delta\varepsilon^2\rangle+\langle(\varepsilon-\langle\varepsilon\rangle)v\xi\rangle\right]$$

which, parallel to *Eq.* 46, can be obtained through simple manipulations from the LE for a free-particle. Here, the second term on the r.h.s. can be written explicitly with the help of[††]

$$\langle v_\xi^3\xi\rangle=\frac{3(k_BT)^3}{m}\gamma\times\left(1-e^{-2\gamma t}\right)\ \ \langle v_\xi^2\rangle=\frac{k_BT}{m}\times\left(1-e^{-2\gamma t}\right)$$

(where $v_\xi=e^{-\gamma t}\int_0^t e^{+\gamma\tau}\xi(\tau)d\tau/m$ is the random component of the velocity), and we obtain the final result in the form[‡‡]

$$\frac{d\langle\Delta\varepsilon^2\rangle}{dt}=-4\gamma\langle\Delta\varepsilon^2\rangle+4\gamma k_BT\times\varepsilon(0)\times e^{-2\gamma t}+2\gamma(k_BT)^2\times\left(1-e^{-2\gamma t}\right)$$

Thus, at short times and for $\varepsilon(0) \gg \varepsilon_{th}$, we find a simple relation between the rate of change of the energy and that of its fluctuations

$$\frac{d\langle\varepsilon\rangle}{dt}\approx-2\gamma\varepsilon\ \ \frac{d\langle\Delta\varepsilon^2\rangle}{dt}\approx 4\gamma k_BT\varepsilon=-2k_BT\frac{d\langle\varepsilon\rangle}{dt}$$

which gives the desired width of the distribution of the random term

$$\langle\zeta^2\rangle=\frac{k_BT}{\varepsilon}\alpha\approx\frac{k_BT}{\varepsilon(0)}\alpha$$

when the same relation is enforced in the quasi-Langevin description outlined above. This shows that α alone determines the quasi-Langevin equation *Eq.* 47 and this can be obtained either from exploratory dynamical simulations involving the lattice or simply estimated ($\alpha^{-1}\sim$ few ps typically).

7.4 | Dissociative chemisorption

Dissociative chemisorption is a particular sticking process in which a molecule colliding with a surface is dissociated and adsorbed as two separated fragments. In the past years, many useful concepts have been developed to understand how the translational, the vibrational, and the rotational degrees of freedom of the molecule come into play in determining the outcome of the reaction (see, for instance, the excellent reviews on the topic of Refs. 62–65). The complex interplay of several factors makes difficult—if not impossible—to derive a simple yet comprehensive model of dissociative chemisorption. Here, we just focus on a specific aspect of the problem, the role that the surface phonons play on the reaction. The latter have been the subject of recent investigations that helped to shed light on general questions regarding the role of surface motion in scattering problems.

From a general perspective, surfaces can be seen to exert two different roles in chemical dynamics. Phonons may play a passive role, in which they act as a large dimensional bath coupled to the reaction coordinate that dissipates the energy of the system and induces thermal fluctuations. In this case, their main effects can be captured with simplified models, since the detail of the lattice dynamics is not relevant and a statistical description suffices for most purposes. At the opposite extreme, phonons may play an active role: the motion of some lattice degrees of freedom, directly coupled to the reaction coordinate, shapes a distortion of the reaction potential which is crucial for the outcome of the process. Here, the detailed coupling potential that determines the distortion would be required, but most often the main effect come from few surface

** Both α and ζ are dimensionless.

†† To the aim of obtaining such results remember that, since ξ is Gaussian, the correlation $\langle\xi(t_1)\xi(t_2)\rangle$ suffices to write high order correlations such as, *e.g.*, the term $\langle\xi(t_1)\xi(t_2)\xi(t_3)\xi(t_4)\rangle$ that appears when expanding $\langle v_\xi^3\xi\rangle$.

‡‡ It follows that $\langle\Delta\varepsilon^2\rangle=(k_BT)^2/2$ holds under equilibrium conditions, in accordance with the standard result $\langle\Delta\varepsilon^2\rangle=c_Vk_BT^2$ where c_V is the heat capacity ($c_V=k_B/2$ in our case).

degrees of freedom, i.e., from those "closest" to the reaction site that are directly involved in the dynamics. Hence, under such circumstances, it is possible to include these effects with larger (but yet attainable) dynamical models.

In general, the surface plays an active role when the dynamics is activated and any tiny lattice deformation may show up in the reaction probability. In this case, fortunately, the passive role of the surface atoms can be neglected, and accurate reduced-dimensional models including the most important surface degrees of freedom developed. This occurs for example in the (activated) dissociative chemisorption of light diatoms (e.g., H_2 on several metal surfaces) since, as is evident from the simple models presented in the previous sections, a large mass mismatch between the projectile and the surface severely limits any energy transfer process.

One of the simplest "active surface" models is the surface oscillator model (SOM),[66,67] in which the molecular Hamiltonian is coupled to a "surface oscillator" through the rigid surface (RS) potential. Specifically, for a diatom *AB* with atom coordinates $\mathbf{r}_A$ and $\mathbf{r}_B$, atom momenta $\mathbf{p}_A$ and $\mathbf{p}_B$ and masses m_A and m_B, the SOM Hamiltonian reads as

$$H=\frac{\mathbf{p}_A^2}{2m_A}+\frac{\mathbf{p}_B^2}{2m_B}+V_S(\mathbf{r}_A-Z\hat{\mathbf{z}},\mathbf{r}_B-Z\hat{\mathbf{z}})+\frac{P^2}{2M_S}+\frac{M_S\Omega_S^2Z^2}{2} \tag{48}$$

where $V_S(\mathbf{r}_A,\mathbf{r}_B)$ is the molecular potential comprising the interaction of the molecule with the *static* surface, $\hat{\mathbf{z}}$ the surface normal, and Z (P) is the height (momentum) of the "surface," taken to be a harmonic oscillator of mass M_S and frequency Ω_s. The rationale here is that the interaction of *AB* with the surface atoms mainly depends on the relative position of the molecule with respect to the average height of the topmost surface layer, i.e. the phonon-molecule coupling is dominated by out-of-plane surface phonons and this effect can be well captured by a single oscillator. The model Hamiltonian of *Eq*. 48 has one additional degree of freedom, but allows one to easily introduce surface temperature and barrier shift effects.[68,69]

Two different limits are worth discussing in this context. One is for $\Omega\to\infty$ where the surface oscillator becomes prohibitively stiff that it does not take part to the dynamics. This is the trivial limit where the dynamics comes back to that of the rigid surface case. The opposite limit for $\Omega\to 0$ is more interesting, since in that case the surface oscillator becomes "free" and plays a simple kinematic role in the dynamics. In this limiting model (also known as surface *mass* model, SMM) the effect of the additional degree of freedom is to convert collision energies ε in energies of the *relative* motion ε_{rel}, according to the mass chosen to represent the surface and the initial speed v_S of the oscillator. As a consequence, the SMM probabilities are simple convolutions of the rigid-surface ones (P_s^{RS}),

$$P_s^{SMM}(\varepsilon,v)=\int P_s^{RS}(\varepsilon_{\text{rel}}(\varepsilon,v_S),v)\,g(v_S)dv_S$$

where $\varepsilon_{\text{rel}}=\frac{1}{2}\mu(v_{AB}-v_S)^2$ (with μ is the reduced mass $\mu^{-1}=(m_A+m_B)^{-1}+M_S^{-1}$ and v_{AB} the COM speed of the molecule along z) and v collectively labels the internal molecular states.

At a more accurate level, one can try to take the effect of some *true* surface oscillators into account, e.g., for the above problem of the diatomics, to consider the Hamiltonian

$$H=\frac{\mathbf{p}_A^2}{2m_A}+\frac{\mathbf{p}_B^2}{2m_B}+V_S(\mathbf{r}_A,\mathbf{r}_B)+\sum_k\frac{p_k^2}{2m_S}+V_L(\mathbf{q})+V_I(\mathbf{r}_A,\mathbf{r}_B,\mathbf{q}) \tag{49}$$

in place of *Eq*. 48. Here, $\mathbf{q}=(q_1,q_2,..)$ [$\mathbf{p}=(p_1,p_2,..)$] are the coordinates [momenta] of the surface degrees of freedom, m_S their mass, and the total potential has been split into three terms: V_S is the above static surface potential, V_L is the lattice potential, and V_I is the coupling between the molecule and the surface degrees of freedom. This is particularly useful when the phonon-molecule coupling is weak and the motion of the projectile is faster than the vibrations of the (heavy) surface atoms, since in this limit a *diabatic approximation* on the q_k's is possible. In other words, during a rapid scattering process the slowly moving surface atoms cannot adjust their position, rather remain essentially frozen in their initial arrangement. Each given lattice configuration determines its own dynamics, and appropriate averaging is needed to wash out such dependence, This vibrational diabatic approximation is also referred to as "Sudden Approximation," and has long been known in gas-phase dynamics, since the pioneering works by Bowman et al.[70,71] In the context of gas-surface scattering is often referred to as Phonon Sudden Approximation (PSA), and its application in classical dynamics is straightforward: the initial position of the lattice atoms are sampled from the equilibrium distribution and molecular trajectories are integrated in accordance with the sudden Hamiltonian

$$H_{\text{PSA}}=\frac{\mathbf{p}_A^2}{2m_A}+\frac{\mathbf{p}_B^2}{2m_B}+V_S(\mathbf{r}_A,\mathbf{r}_B)+V_I(\mathbf{r}_A,\mathbf{r}_B|\mathbf{q}) \tag{50}$$

where the vertical bar has been introduced in V_I to emphasize that the dependence of the potential on the q_k's is only parametric. In other words, as mentioned above, the lattice coordinates are frozen during the dynamics, with values chosen randomly from the appropriate distribution. This classical approach has been successfully applied, for instance, in Ref. 72 to estimate the *static* effect of surface temperature on the dissociative chemisorption probabilities of H_2 and D_2 on Cu(111).

The above Phonon Sudden Approximation can be generalized to a quantum setting, upon assuming that the coupling potential does not affect the evolution of the lattice dynamics, i.e. that

$$[H_L,V_I]\approx 0 \tag{51}$$

approximately holds, $H_L=\sum_k\frac{p_k^2}{2m_S}+V_L(\mathbf{q})$ being the lattice Hamiltonian. Under these conditions, the scattering amplitude for the collisional transition $(v,\mathbf{i})\to(v',\mathbf{f})$ between the v and v' molecular states and the $\mathbf{i}$ and $\mathbf{f}$ surface states (they are all multiindex) can be obtained by integrating the PSA scattering matrix, namely from

$$S^{\text{PSA}}(v',\mathbf{f}\leftarrow v,\mathbf{i})=\langle\mathbf{f}|s^{\text{PSA}}(v'\leftarrow v|\mathbf{q})|\mathbf{i}\rangle \tag{52}$$

where $s^{\text{PSA}}(v'\leftarrow v|\mathbf{q})$ is the solution of the scattering problem defined by the sudden Hamiltonian, *Eq*. 50, with the lattice coordinates fixed at $\mathbf{q}$. The full knowledge of $s^{\text{PSA}}(v'\leftarrow v|\mathbf{q})$, allows one to compute the state-to-state scattering probabilities, which are the square of the

scattering matrix elements, for any initial and final state, just by performing the quadrature of *Eq.* 52.

In general, given the state resolved scattering amplitude $S(v', \mathbf{f} \leftarrow v, \mathbf{i})$, the initial-state-selected dissociative adsorption probability follows as

$$P_s(v, \mathbf{i}) = 1 - \sum_{v', \mathbf{f}} |S(v', \mathbf{f} \leftarrow v, \mathbf{i})|^2 \tag{53}$$

where the sum runs over all internal state of the molecule and the states of the lattice[§§]. Plugging the PSA scattering amplitude in the above expression gives the corresponding probability in the phonon sudden approximation

$$P_s^{\mathrm{PSA}}(v, \mathbf{i}) = 1 - \sum_{v', \mathbf{f}} \langle \mathbf{i} | s^{\mathrm{PSA}}(v' \leftarrow v|\mathbf{q})^\dagger | \mathbf{f} \rangle \langle \mathbf{f} | s^{\mathrm{PSA}}(v' \leftarrow v|\mathbf{q}) | \mathbf{i} \rangle$$

$$= \langle \mathbf{i} | p_s^{\mathrm{PSA}}(v|\mathbf{q}) | \mathbf{i} \rangle = \int d^F\mathbf{q} |\Phi_i(\mathbf{q})|^2 p_s^{\mathrm{PSA}}(v|\mathbf{q}) \tag{54}$$

where

$$p_s^{\mathrm{PSA}}(v|\mathbf{q}) = 1 - \sum_{v'} |s^{\mathrm{PSA}}(v' \leftarrow v|\mathbf{q})|^2$$

and $\Phi_i(\mathbf{q})$ is a bath eigenfunction. *Equation* 54 is a simple statistical average, since no phase factor is present in p_s^{PSA}. As a consequence, in analogy with classical dynamics, the PSA dissociative chemisorption probability is simply the average of the probability at fixed lattice coordinates, weighted by an appropriate distribution $|\Phi_i(\mathbf{q})|^2$, a rather physically sound result. We notice though that the manipulation leading to *Eq.* 54 is rather subtle since it implicitly assumes that the computed scattering matrices are made *non-unitary* in practice (e.g., by imposing absorbing potentials).

8 | APPLICATIONS

So far we have presented the general phenomenology of processes at surface, along with those basic concepts that allow a "zeroth order" description of the dynamics. We close this review with a brief overview of real world systems, since recent years have witnessed a great progress in atomistic simulations that a close comparison with experimental findings has been possible in many cases. Such progress is the result of a virtuous interaction between the availability of powerful computational resources and the development of accurate and reliable methodologies. The focus of this review is on the dynamics, but the advances in electronic structure theory played such an important role that can hardly be overemphasized. We just mention that Density Functional Theory definitely emerged as a thoroughbred, and DFT methods have been made available to compute interaction energies in the chemical range (including the van der Waals realm) for systems of the typical size necessary in many surface science problems. As for the dynamics, the situation is less distinct and a large number of complementary approaches have emerged from the variety of challenges presented by surface science. They are schematically depicted in Figure 7, and briefly introduced in the following.

The simplest and most straightforward approach is to treat the projectile and a variable portion of the surface with classical molecular dynamics. At this level, (mechanical) environmental effects can be safely assigned to the lattice boundaries and thus described by Langevin forces acting on the edge atoms only. The obvious advantage of classical dynamics is the low cost of propagation that allows the introduction of a large number of degrees of freedom or the use of high-quality information on the interactions (such as on-the-fly *ab initio* computation of the forces).

At the opposite extreme, there are approaches in which both the scattering particle and the lattice are treated at a quantum level. In this case, a "brute force" approach in which both are explicitly considered in detail is out of reach because of the well known exponential scaling of quantum dynamics. One viable route in this case is to extract a primary system (called simply the system) that contains the most relevant degrees of freedom (usually the projectile plus possibly some strongly coupled lattice coordinates). If necessary, the effect of the environment on the system can be incorporated at a fully quantum level with open-system quantum techniques, e.g. master equations for the reduced density operator of the system or system-bath unitary dynamics.

Between these two extremes, there lies a variety of models in which *ad-hoc* approximations are exploited to study a particular aspect of the scattering problem. In many "small quantum system" approaches, the fully quantum description of the scattering dynamics is retained at the expense of an arbitrary reduction (or even neglect) of the lattice degrees of freedom. Two examples are the above mentioned Surface Oscillator model and Phonon Sudden Approximation that aim at capturing some specific aspects of the dynamical effect of the surface. On the contrary, when the quantum nature of the lattice is preserved at the expense of the scattering coordinates, we have methods based on the Forced Oscillator Model, which was conceived to study with accuracy the energy transfer to the lattice.

Inclusion of e-h excitations, when needed, is straightforward only if the system dynamics is treated classically and an electronic friction is used, otherwise it requires ad hoc (modelistic) modification to the above described approaches.

In this final section, we present a few examples of both quantum and classical studies in the field of surface science, chosen to illustrate some typical problems and the adopted theoretical approach. The list does not claim to be exhaustive nor definitive, rather follows the interests and the expertise of the authors.

8.1 | Classical dynamics

We start our short examination from the molecular dynamics study by Shalashilin and Jackson on H scattering from Cu(111),[61] who demonstrated the efficacy of a combined use of standard trajectories and advanced stochastic models. In this work, a large slab of 150 Cu atoms was used to investigate the behavior of hot-atoms on a dynamic lattice, and forces were computed with a reasonable analytical potential. The

[§§] If needed, these quantities can be averaged over the thermal distribution of the bath states to give the probability at given surface temperature, $P_s(v, T) = \sum_i p_i(T) P_s(v, \mathbf{i})$.

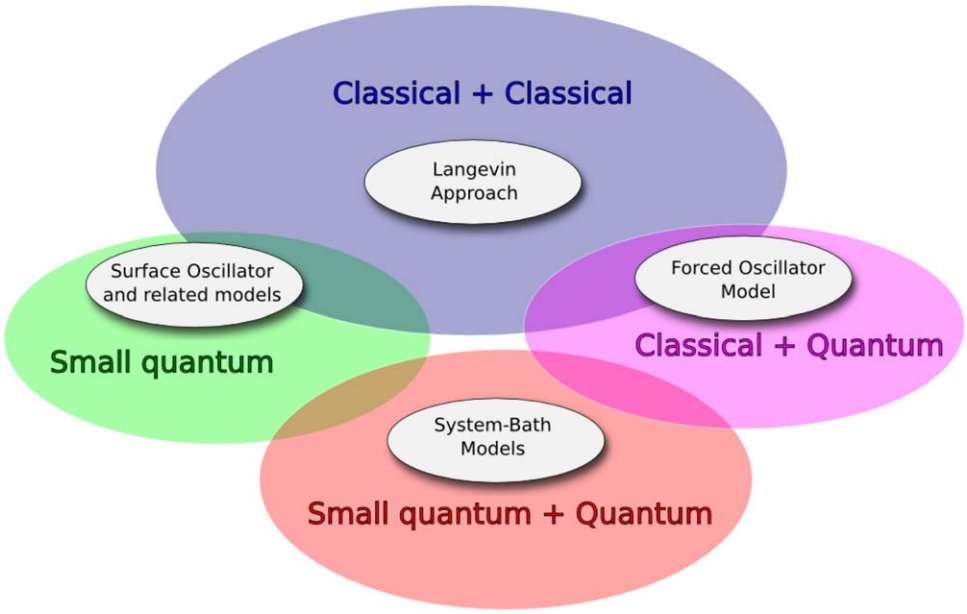

FIGURE 7 A cartoon illustrating several dynamical schemes adopted to handle gas-surface dynamical problems

formation of trapped hot species was analyzed in detail, as well as the nature of their motion on the surface and their energy and momentum dissipation. Furthermore, the results were scrutinized for a Fokker–Planck description of the slow energy decay process, which was then used to build a satisfactory "quasi-Langevin" description of the atom dynamics based on the rigid-surface potential only. As mentioned in section "Reactions—Hot Atoms," the difference with the standard Langevin approach consists in the structure of the friction and fluctuating forces, which were designed to describe the small energy transfer of the light atoms to the surface. The model as such is in fact readily extended to include electronic friction effects, which have been recently found substantial in some hot-atom dynamics.[35] Adsorbate-induced HA formation and (phonon mediated) stabilization of hot hydrogen atoms were also investigated in Ref. [73], where a detailed comparison of Eley–Rideal reaction and Hot-Atom formation was performed for hydrogen atoms recombining on Ni(100). The authors of Ref. [73] used an accurate Embedded Diatomics in Metal potential model [74]—a variant of the popular Embedded Atom Method[75,76]—and a large slab (9×9×11) to follow the dynamics of projectile H atoms fired on a previously covered Ni(100) surface. They found that hot-atom formation cross-sections are much larger than ER ones, and that both the adsorbate-induced corrugation and the enhanced energy transfer with the (light) targets play a role in forming *stable* hot species already at the first impact. Figure 8 shows an example of the simulation results which is illustrative of the hot-atom properties: there is plotted the energy distribution of the trapped species after about 1 ps at a surface temperature of $T=120$ K, for different values of the collision energy (the curves would slowly shift toward lower energy since HA relaxation was found to occur on a time scale of $\sim$ 4–5 ps).

Recently, the advent of large and fast supercomputing facilities has opened the way to Ab Initio Molecular Dynamics (AIMD), with Density Functional Theory forces computed on-the-fly. While this methodology ensures that the forces are accurate and reliable, it requires a much more expensive evaluation of the forces, when compared to standard molecular dynamics. As a consequence, a tradeoff has often to be found between the size of the simulation cell and the quality of the statistics. Nevertheless, high quality results can already be obtained by judiciously choosing the set up for running AIMD. Nattino et al.,[77] for instance, investigated methane dissociative chemisorption on Pt(111) and used a 3 × 3 surface unit-cell slab with 5 atomic layers to model the surface. These 45 platinum atoms were proven to be enough to capture the active effects of the lattice motion which were most important in dissociating the molecule. The authors of Ref. [77] investigated in detail a number of issues, including the dependence of the reaction probabilities on the initial vibrational state of the molecule, its rotational alignment, and the temperature of the surface. They further performed a thorough comparison with available experimental results at a quantitative level, thereby demonstrating the power of this methodology.

AIMD was also used to investigate relaxation of hot atoms resulting from molecular dissociation, as mediated by both phonon excitation and electronic friction.[35] The aim of the authors of Ref. [35] was to establish at what stage of the dissociation of a molecule *e–h* pair excitation becomes relevant, in light of the contradicting evidences that an adiabatic picture seems to work in most cases for dissociative chemisorption but electron excitations are indeed observed during reactions, as e.g. chemicurrents. The findings of Ref. 35 point towards a primary role of *e–h* pair excitations in hot atom relaxation, a result that might be exaggerated by the rather crude description of the electronic friction (the local density friction approximation, see "Energy Transfer—Electronic friction")*** but does prove the ubiquitous role of electronic excitations when dealing with metal surfaces. Notice, further, that the hot-species

*** Indeed, in LDFA the friction is entirely determined by the value of the electron density at the atom position. Hence, also insulating surfaces would be effective in providing such friction.

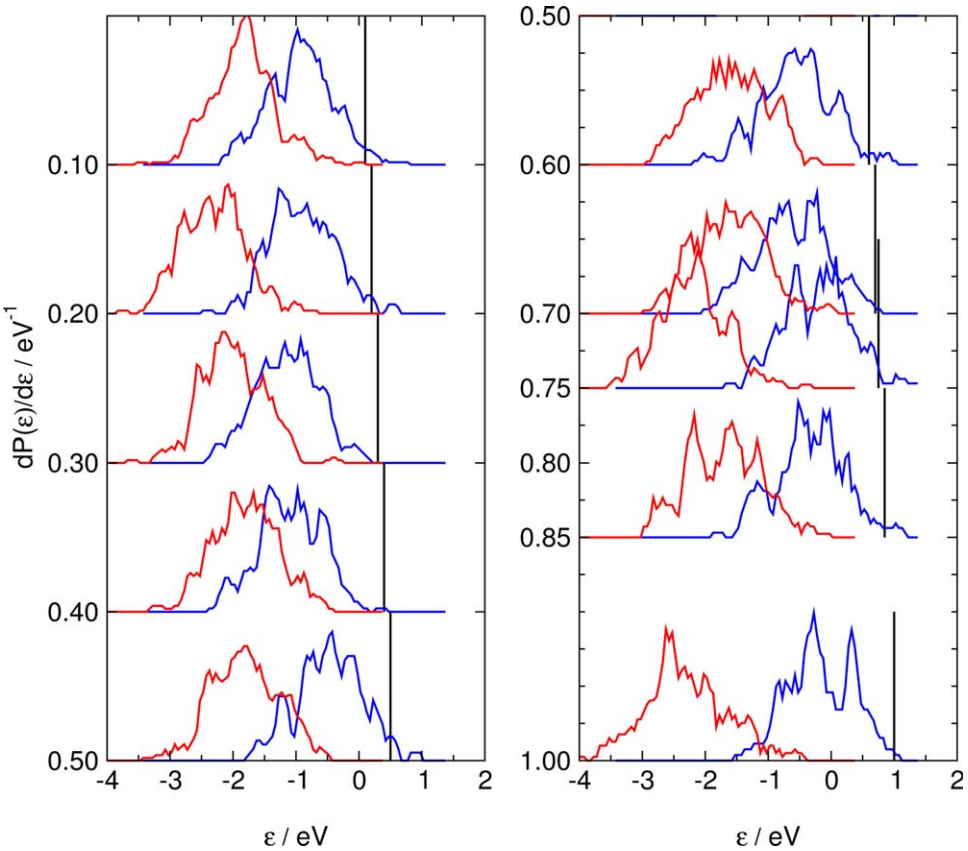

FIGURE 8 Energy distribution of hot hydrogen species formed on a Ni(100) surface at T= 120 K, pre-covered with H atoms, ~1 ps after the impact on an occupied (red) or empty (blue) adsorption site. The different values of the collision energies are indicated on the ordinate axis and by the small vertical bars, and the zero of energy has been aligned with the desorption threshold. Reprinted from R. Martinazzo, S. Assoni, G. Marinoni and G.F. Tantardini, J. Chem. Phys. 120, 8761 (2004) with the permission of AIP Publishing

formed in such a molecular dissociation process are sensitively slower than those obtained when firing atomic species at a surface, hence the HA energy distributions are colder than those shown in Figure 8 and correspondingly the traveled are typically much shorter distances than those mentioned above, at the beginning of this Section.

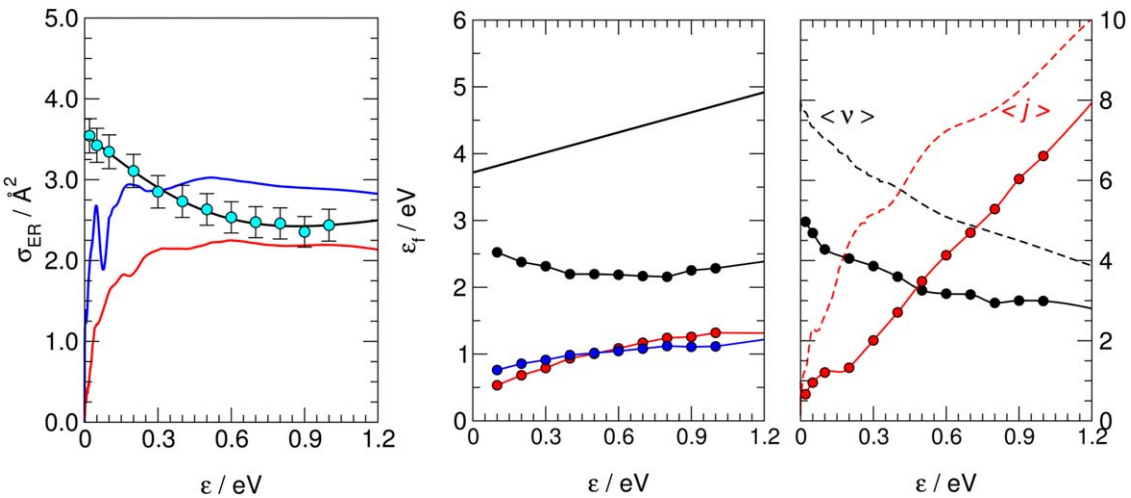

FIGURE 9 Results of an AIMD investigation of the Eley–Rideal formation of H_2 on graphite. Left panel: cross-sections for ER recombination from AIMD (dots with error bars) and from quantum calculations within the adiabatic (blue) and sudden (red) rigid, flat-surface models (see the main text). Middle: partitioning of the reaction energy into surface degrees of freedom (blue), H_2 translational energy (red), and H_2 internal energy (black). The black line shows the total energy available (the reaction exothermicity plus the collision energy). Right panel: average H_2 vibrational (black) and rotational (red) quantum numbers as obtained through standard binning of the AIMD results (dots-full lines) and from quantum calculations (dashed lines). Adapted with permission from S. Casolo, G. F. Tantardini and R. Martinazzo, J. Phys. Chem. A (2016), in press (DOI: 10.1021/acs.jpca.5b12761). Copyright 2016, American Chemical Society

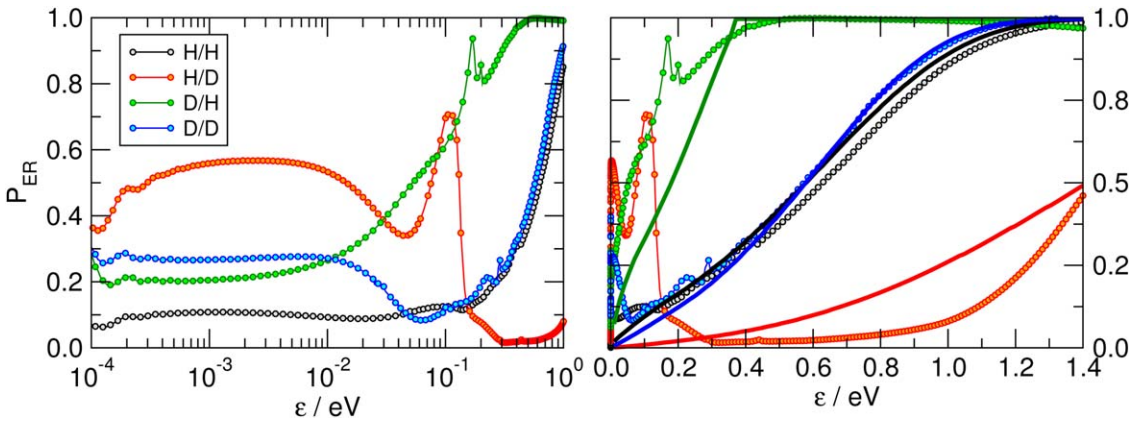

FIGURE 10 ER recombination probabilities from 2D collinear calculations with the adiabatic model, as a function of the collision energy in both log (left panel) and linear (right panel) scales. In the right panel the thick lines are the results of the quasi-classical impulsive model described in the main text, color coded as the quantum results

AIMD was further used in cases of systems strongly coupled with the lattice, such as the Eley–Rideal formation of H_2 on graphitic/graphenic surfaces. The coupling in this case arises from the fact the adsorbed H atom forms a strong, covalent bond with one atom of the lattice, and its breaking may leave substantial energy into the substrate. In fact, since the C atom is sp^3 hybridized and protrudes from the flat surface, after reaction it can be found in a highly excited vibrational state. This and other issues (e.g., the competing formation of dimers on the surface) have been described by Casolo et al.,[78,79] who performed a detailed comparison between classical and reduced-dimensional quantum studies, and with available experimental data. The results of Refs. [78,79] show that Eley–Rideal reaction dominates over dimer formation at collision energies relevant for the chemistry of the interstellar medium, thereby ruling out possible catalytic pathways in H_2 formation that involve dimers on the surface. They further show that reaction is accompanied by substantial substrate heating: formation of a single H_2 molecule may rise the surface temperature of a typical (μm-sized) interstellar grain by 2×10^{-4} K. Figure 9 shows some illustrative results of these studies: reaction cross-sections, energy partitioning and (average) rotational, and vibrational quantum numbers for the product H_2 (obtained by standard binning of the trajectory results). One striking feature evident from this figure is the size of the cross-sections which, despite the unfavorable $\frac{1}{4}$ spin-statistical factor which had to be corrected for, are much larger than $\sim$1 Å^2 typical of Eley–Rideal recombination on metal surfaces, as discussed previously in section "Reaction—Eley–Rideal." Also evident in Figure 9 is the internal excitation of the product molecules, a rather common feature that follow from the exothermicity and the specific mechanism of the reaction (see Section "Reaction—Eley–Rideal"); in particular, the opposite behavior of the vibrational and rotational excitation vs. energy (right panel) signals the competition between head-on and glancing collisions in determining the reaction outcome.

8.2 | Quantum dynamics

Eley–Rideal H_2 formation on graphene is also one of the most studied *quantum* scattering problems. In this context, the description is often simplified by invoking the rigid and flat surface approximation, i.e. assuming that the lattice is frozen and neglecting the corrugation of the atom-surface potential. As a consequence, the total momentum parallel to the surface and the projection of the total angular momentum on the surface normal are conserved quantities and the overall description includes three degrees of freedom only.[80] In light of the strong coupling between the previously adsorbed hydrogen and the bonding carbon, the role of the substrate atom is often statically included in the potential energy surface, considering two different (opposite) limiting behaviors[81,82]: either with a sudden approximation or with an adiabatic approximation. In the first case, the reaction dynamics is supposed to be so fast that the C atom remains frozen in its reconstructed configuration, whereas in the second case the substrate atom relaxes instantaneously during the supposedly slow recombination process. A comparison of the results obtained in these two

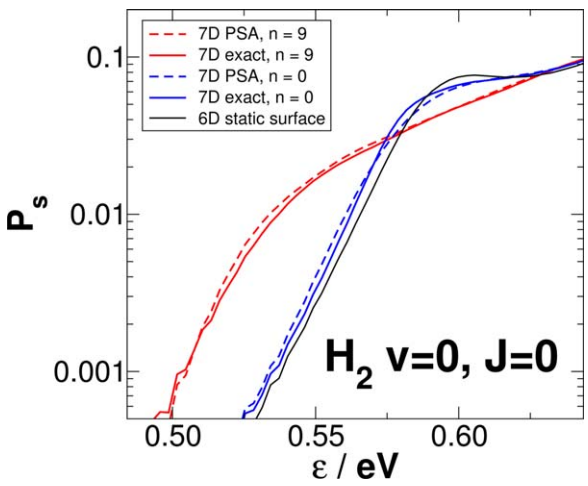

FIGURE 11 Dissociative chemisorption probability as a function of the collision energy for state-selected H_2 scattering off the Cu (111) surface. The rigid-surface 6D quantum results (black) are compared with exact 7D quantum calculations (thin blue and red lines) and 7D calculations using the phonon sudden approximation (dashed lines). *n* is the vibrational quantum number of the additional surface mode included in the 7D calculations

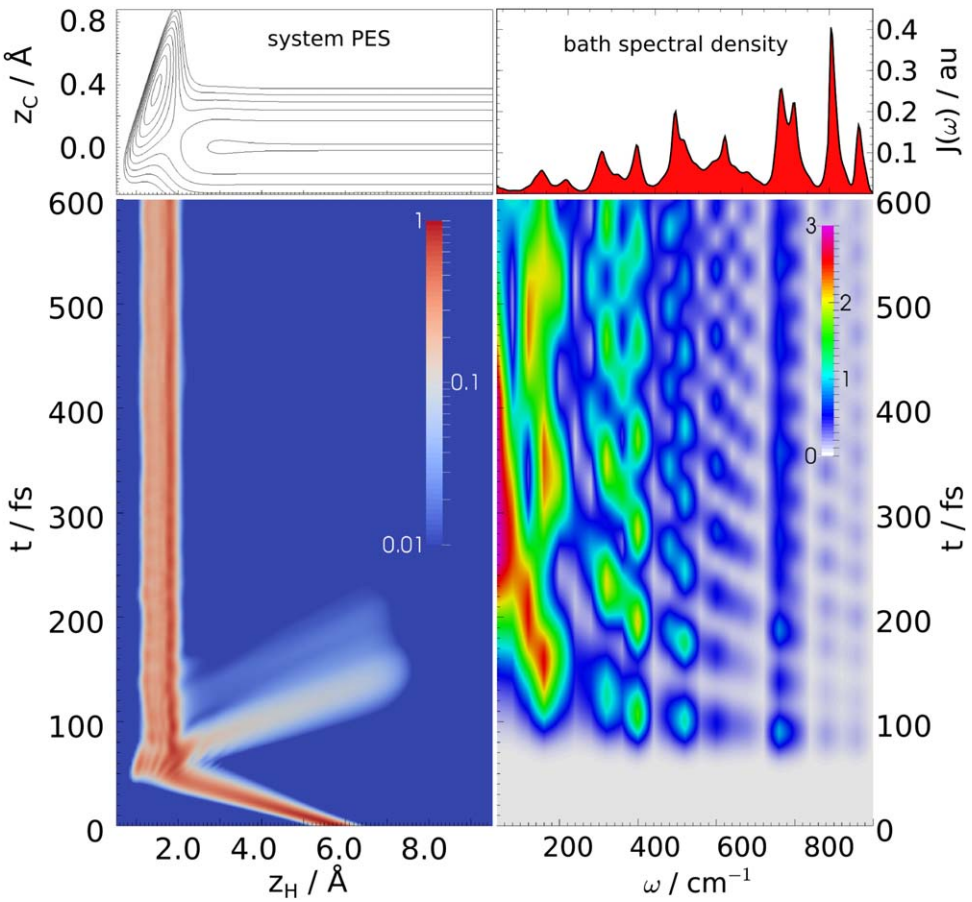

FIGURE 12 Time evolution of the reduced density along the height of the hydrogen atom above the surface (z_H, left bottom panel) and of the average excitation number of the bath oscillators (right bottom panel) in a typical high dimensional quantum simulation. The average initial momentum was 7 a.u., corresponding to a nominal collision energy of 0.36 eV. The top panel on the left shows a contour plot of the system potential aligned along z_H, and the top panel on the right gives the spectral density $J_C(\omega)$ felt by the binding C atom, in correspondence with the bath oscillator frequency. Reprinted from M. Bonfanti, B. Jackson, K.H. Hughes, I. Burghardt and R. Martinazzo, J. Chem. Phys. 124704 (2015) with the permission of AIP Publishing

limits is given in Figure 9, along with the AIMD results, where it is shown that they provide reliable upper and lower bounds to the cross-sections, at least in the regime where classical mechanics is valid. Several aspects have been scrutinized on the quantum dynamics of H_2 formation on graphite—e.g., the internal excitation of the products, the quantum effects at high energies and the cold collision energy dynamics, the isotope effects, etc.—and novel methodologies developed to overcome problematic issues.[58,83,84] The reader is referred to the original literature[58,82,84–87] and review articles.[88] Here, we rather focus on the simple collinear dynamics, which is illustrative of the concepts developed in section "Reactions—Eley–Rideal." Figure 10 shows that the ER reaction presents a marked isotopic dependence in these head-on collisions. At high energy, where the dynamics is classic, the behavior of the probability curves is well-captured by the simple, quasi-classical impulsive models described above. The only necessary adjustment is in the target atom velocity distribution function: in this case the impulsive limit does not strictly holds, since the target atom performs few vibrations during the collision. To remedy this deficiency, we can assume that the average kinetic energy increases by D_{eff} due to the interaction with the projectile while the momentum distribution keeps the same shape and average. This amounts to replace the original target frequency ω_S (determining the momentum wavefunction $\phi_v(p)$) with an effective frequency $\omega_{\text{eff}}=\omega_S+4D_{\text{eff}}/\hbar$. The results of these quasi-impulsive models—shown in Figure 10 as full lines—capture rather well the main aspects of the dynamics at a moderate-to-high collision energies. At smaller ("cold") energies, the reaction probability shows a general decrease despite the absence of any reaction barrier, but the detailed behavior is hardly rationalizable and likely bound to the details of the interaction potential. This is the quantum regime where quantum reflection and dynamical resonances play a primary role.

The Phonon Sudden Approximation has been introduced and tested by the authors of Ref. [89], who used the dissociative chemisorption of H_2 on Cu(111) as a testing ground for this approximation. Here, an additional degree of freedom for the motion of a lattice coordinate was added to the dynamical description that, in turn, became a seven-dimensional model. Quantum wave-packet propagation was used to compute reaction and state-to-state scattering probabilities.

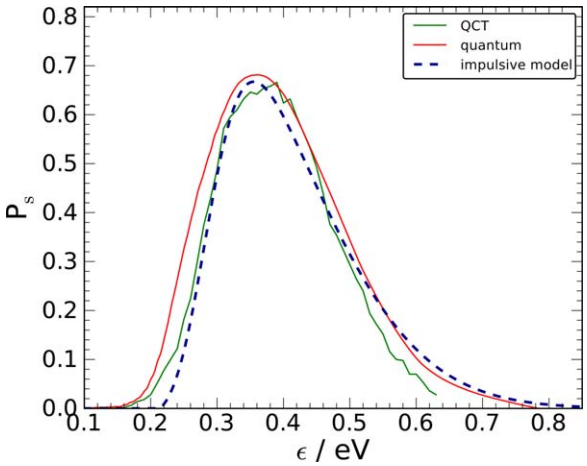

FIGURE 13 H atom sticking probability on graphene from quasi-classical (green) and quantum (red) calculations, compared with the results of an impulsive model using the quantum distribution of the surface atom velocities (dashed lines). See main text for details. Reprinted from M. Bonfanti, B. Jackson, K.H. Hughes, I. Burghardt and R. Martinazzo, J. Chem. Phys. 124704 (2015) with the permission of AIP Publishing

For instance, in Figure 11 the sticking probability is shown as a function of the incidence energy of a molecule in the rovibrational ground state $v = 0$, $J = 0$, for different states of the substrate. Because of the small coupling between the molecule and the phonons of the surface, the sticking curves for the vibrational ground state of the lattice coordinate ($n = 0$) differ only slightly from the one with the static surface, i.e. kept fixed in the equilibrium position. A significant increase of the reaction probability at the threshold energy was found however when the lattice was vibrationally excited ($n = 9$). The graph shows that for both vibrational states the exact 7D calculations and the PSA results are in excellent agreement. It has been established, in fact, that in H_2 scattering off Cu(111) the role of the surface is almost perfectly captured already at a static level, by taking into account the distortion of the potential induced by the thermal fluctuations of the lattice atoms.

Vibrational relaxation was investigated within and beyond the Fermi-golden-rule approximation described in Section "Vibrational Relaxation." Saalfrank and coworkers, for instance, investigated in detail the relaxation dynamics of H atoms stuck on the Si(100) surface, and the competition with laser-field excitation in producing mode (state) selective products.[90,91] In a thorough analysis of the H—Si(100)-2×1 system, they developed a microscopic model describing Si—H bending and stretching, and their anharmonic coupling to the Si lattice. Using the Fermi-golden-rule to compute the vibrational lifetimes τ and including one- and two-phonon decay processes, as well as anharmonic coupling in the Si—H vibrations, they rationalized the striking differences between the bending ($\tau\sim$ ps) and the stretching ($\tau\sim$ ns) lifetimes.[90] They found that, even though both vibrational modes have frequencies well above the Debye frequency of the Si substrate, only the bending mode is capable of exciting two surface phonons and thus relax on a ps timescale. The stretching mode could only relax *via* anharmonic coupling to the bending, i.e. through creation of two bending quanta for each quantum put in the stretching mode. This study was later extended[91] beyond the Markov regime implicitly assumed in adopting a rate description, and the fast relaxing bending mode explicitly followed in real time with high dimensional wavepacket simulations of the Multi-Configurational Time-Dependent Hartree (MCTDH) type.[92–94] Interestingly, the effect of the surface temperature was investigated via an efficient stochastic representation of the thermal density operator[95] and found to substantially reduce the lifetime of the vibrationally excited species adsorbed on the surface.[91]

To the best of our knowledge, the only numerically converged, fully quantum study of a strongly coupled scattering problem, explicitly including the lattice degrees of freedom, is our recent work on the activated dynamics of hydrogen sticking on a graphitic/graphenic surface.[36,96] This has been possible upon exploiting the relation between the independent oscillator models and the Langevin dynamics discussed in Appendix. We have devised and applied an elaborate strategy which, starting from the development of a general technique to extract information on the environmental forces acting on the system[47] and the definition of a suitable dynamical model for a H atom bound to graphene,[96] allowed us to investigate the sticking dynamics in a fully quantum setting.[36]

Briefly, the model includes an accurate description of the hydrogen atom and its bonding carbon atom that, in turn, is linearly coupled to a bath of harmonic oscillators mimicking the graphene sheet. The inclusion of the carbon in the primary system is motivated by the large reconstruction that the surface undergoes during the sticking process. This simplified yet faithful description was successfully studied with converged MCTDH calculations,[92–94] with a focus on the collinear scattering dynamics on a zero-temperature surface. An overview of a typical dynamical simulation is reported in Figure 12, which displays the time evolution of the probability density along z_H, the height of the projectile H atom above the surface. The figure clearly shows that when the scattering wavepacket approaches the surface a small fraction is directly reflected while the largest fraction overcomes the barrier and reaches the adsorption well. At a later time (in few tens of fs), a further fraction is expelled and constitutes the inelastically scattered probability. The rest of the wavepacket remains *trapped* in the adsorption well and relaxes. The right panel of Figure 12 gives the corresponding time-evolution of the bath excitation, represented as the average occupation number of the oscillators (average number of phonons). Excitation first involves the high frequency modes only but in a rather short time interval spreads over the whole frequency range, as a consequence of the strong coupling between the bath and the surface phonons.

By combining the energy resolved results of several wavepacket simulations, we computed the quantum mechanical sticking probability curve illustrated in Figure 13. For comparison, also reported are the results of zero-temperature quasi-classical simulations of the dynamics, which are seen to be in remarkably good agreement with the quantum ones (except for the threshold region where tunneling dominates), in sharp contrast with the purely classical results. This highlights the importance played by the zero point fluctuations of the lattice, which are necessary to achieve a reasonable description of the sticking process.

Both quantum and quasi-classical curves shows the two contrasting behaviors described in section "Sticking" for the impulsive model of activated adsorption. At incidence energies around E_b (~0.2 eV in this case), the process is limited by the probability that the projectile atom overcomes the barrier, since any H atom that reaches the interaction region is able to dissipate the small amount of energy in excess to get trapped. As a consequence, in this regime P_s grows with increasing collision energy. On the contrary, at higher collision energy the sticking probability decreases. In this case the atoms have always enough energy to reach the chemisorption well, but sticking only occurs if energy relaxation is efficient enough to prevent the projectile to re-cross the barrier and return to the gas-phase. This analysis is supported also by a quantitative use of the impulsive approximation. Fitting the quasi-classical model introduced in section "Sticking" to the simulation results, we obtained quite a good representation of the sticking probability (see Figure 13, dashed line), with reasonable values of the model parameters.[36]

9 | CONCLUDING REMARKS

We presented a simplified overview of some basic dynamical phenomena involving atoms or molecules and solid surfaces, with an emphasis on those models that elucidate the main physics governing the elementary processes. This allowed us to single out key dynamical factors and to identify relevant regimes and appropriate length and time scales. These concepts form the basis for understanding real-world dynamical phenomena, which most often show a much richer behavior than the one outlined here, thanks to the combination of molecular and surface complexity, and to the pecularities of the gas-surface interactions. The concepts developed here are though essential for extracting genuine aspects of specific molecule-surface pairs and may be of help in unraveling new dynamical behaviors.

ACKNOWLEDGMENTS

This work has arisen over the years through an intense and fruitful collaboration with several people. Among them, the authors are particularly in debt to Gian Franco Tantardini, who introduced us to the field, and to Peter Saalfrank, Mathias Nest, Geert-Jan Kroes, Simone Casolo, Didier Lemoine, Mark Somers, Bret Jackson and Francesco Nattino. They are all sincerely acknowledged for the contribution they gave to our understanding of several fascinating phenomena occurring at surfaces, and for the pleasant time we spent together.

APPENDIX : LANGEVIN DYNAMICS AND OSCILLATOR MODELS

In the main text we have seen that a number of oscillator models naturally arise when considering a particle interacting with a surface. Their popularity stems from the fact that, if properly defined, they relate a microscopic (Hamiltonian) description to a reduced-dimensional (dissipative) setting of the dynamics,[41] that provided by the Generalized Langevin Equation of motion,[40,41,97]

$$m\ddot{z}(t)+m\int_{-\infty}^{t}\gamma(t-\tau)\dot{z}(\tau)d\tau+V'(z(t))=\xi(t) \tag{A.1}$$

and its memory-less limit, the Langevin equation

$$m\ddot{z}(t)+m\gamma\dot{z}(t)+V'(z(t))=\xi(t) \tag{A.2}$$

In *Eq. A.1*, a particle of mass m and coordinate z is subjected to a deterministic force $-V'(z)$ and to dissipative and fluctuating forces from the environment. The latter are subsumed in a memory kernel $\gamma(t)$ ($\gamma(t)=2\gamma\delta(t)$ to obtain *Eq. A.2*) and in a stationary stochastic process $\xi(t)$, which are related to each other (fluctuation–dissipation theorem): equilibrium is attained if fluctuating and dissipative forces balance each other.[40,98] In formulas

$$\langle\xi(t_1)\xi(t_2)\rangle=mk_BT\gamma(|t_1-t_2|) \tag{A.3}$$

holds in classical mechanics (the quantum version takes a slightly more complicated form). The GLE provides a unified description of several phenomena, and thus represents a successful microscopic model of dissipation. For instance, when the point particle is subjected only to the effects of the environment ($V\equiv 0$), the GLE above describes free diffusion at sufficiently long times; when $V(z)$ is the periodic surface potential, or one of its cuts through neighboring sites, *Eq. A.1* describes particle escape from one adsorption site to the next one; similarly, when $V(z)$ is the adsorption profile, the GLE can be used to investigate vibrational damping (in linear regime).

In the following, we briefly discuss the relationship between *Eq. A.1* and the independent oscillator model (IOM),[97,99] since this sheds light on the microscopic origins of dissipation and on the emergence of classicality. This is also instrumental for quantum applications (such as those described in section Applications), which in many instances rely on such a relation to describe quantum dissipation with a Hamiltonian dynamics. In the IO model the point particle of coordinate z is subjected to the potential $V(z)$ and is bilinearly coupled to a set of harmonic oscillators

$$H_{IO}=\frac{p_z^2}{2m}+V(z)+\sum_{k=1}^{F}\left[\frac{p_k^2}{2m_k}+\frac{m_k\omega_k^2}{2}\left(q_k-\frac{c_k}{m_k\omega_k^2}z\right)^2\right] \tag{A.4}$$

The particular form of H_{IO} (which "corrects" the potential actually acting on the system, $V(z)\rightarrow V(z)+\delta V(z)$, where $\delta V(z)=z^2\sum_k c_k^2/2m_k\omega_k^2$) guarantees the thermodynamic stability of the model[97]: if $V(z)$ is a reasonably well-behaved potential supporting an energy spectrum bound from below, so is the full Hamiltonian H_{IO} (as is evident from the fact that the "environment"—the sum over the IO modes—adds purely positive terms only). The Hamiltonian of *Eq. A.4* gives rise [in both the classical and the quantum (Heisenberg) setting] to a GL-like equation in which $\gamma(t)$ and $\xi(t)$ are determined by the IO parameters m_k, ω_k^2 and the coupling coefficients c_k. This follows from the Hamilton's equation of motion upon integrating the oscillators degrees of freedom, and picking the bath initial conditions (in the infinite past) from the appropriate equilibrium distribution.[41,98]

Conversely, given a GLE with some memory kernel $\gamma(t)$ one can choose the IO parameters and the coupling coefficients in such a way that H_{IO} describes the same dynamics as the GLE. In other words, there exists an equivalence between the Hamiltonian description of *Eq. A.4* and the GLE of *Eq. A.1*. It holds for *finite* times only, $t<t_P$, since beyond

the so-called Poincaré recurrence time t_P, finite-size effects necessarily show up in the Hamiltonian dynamics. t_P is determined by the bath size (more precisely, $t_P \sim 1/\Delta\omega$ where $\Delta\omega$ is the average frequency spacing) and, in practical applications, needs to be set larger than any time scale of interest in the dynamics.

The "translator" between the two descriptions is usually chosen to be the spectral density of the coupling $J(\omega)$.[41] For the IO Hamiltonian it is defined as

$$J(\omega) = \frac{\pi}{2}\sum_k^F \frac{c_k^2}{m_k\omega_k}\delta(\omega-\omega_k) \tag{A.5}$$

whereas for the GLE it reads as

$$J(\omega) = m\omega\Re\tilde{\gamma}(\omega) \quad \tilde{\gamma}(\omega) = \int_{-\infty}^{\infty}\gamma(t)e^{i\omega t}dt \equiv \int_0^{\infty}\gamma(t)e^{i\omega t}dt \tag{A.6}$$

where use has been made of the *causality* of the memory kernel ($\gamma(t)=0$ for $t<0$). Causality is a key property, since it has important implications for the analyticity of $\tilde{\gamma}$: with the replacement $\omega \to z$ ($\Im z>0$) the "Fourier-Laplace" integral in *Eq. A.6* is indeed a very well-behaved function of z, which means that $\tilde{\gamma}$ can be analytically continued to the whole upper half complex-plane (uhp). In turn, analyticity can be exploited to write down the celebrated Kramers–Kronig relations, and $\tilde{\gamma}(z)$ (for arbitrary z in the uhp) can be represented solely in terms of $\Re\tilde{\gamma}(\omega)$, $\omega \in \mathbb{R}$ (or, equivalently, $\Im\tilde{\gamma}(\omega)$). This shows why knowledge of $J(\omega)$ is *equivalent* to the knowledge of $\gamma(t)$. Furthermore, since $\xi(t)$ appearing in *Eq. A.1* is a Gaussian process, it is fully determined by the correlation $\langle\xi(t)\xi(0)\rangle_\beta$, hence by $\tilde{\gamma}(\omega)$ (by virtue of the fluctuation–dissipation theorem). As a consequence, $J(\omega)$ alone *fully defines* the GLE of *Eq. A.1* for a given $V(z)$, and this explains why the spectral density of the coupling plays such a key role in the description of dissipative systems.

In closing this Appendix, we notice that using a densely set of uniformly arranged frequencies $\omega_k = k\Delta\omega$ ($k=1,..,F$) in *Eq. A.5*, we can write

$$J(\omega) = \frac{\pi\Delta\omega}{2\Delta\omega}\sum_k^F \frac{c_k^2}{m_k\omega_k}\delta(\omega-\omega_k) \approx \frac{\pi}{2\Delta\omega}\int_0^{F\Delta\omega}\frac{c\prime^2}{m\prime\omega\prime}\delta(\omega-\omega\prime)d\omega\prime = \frac{\pi}{2}\frac{c(\omega)^2}{\Delta\omega\, m(\omega)\,\omega}$$

hence the choice

$$c_k = \sqrt{\frac{2m_k\omega_k\Delta\omega_k J(\omega_k)}{\pi}} \tag{A.7}$$

defines a practical way to "sample" a given spectral density and, thus, to map, in practice, a given GLE into an IO model.

How to cite this article: M. Bonfanti, R. Martinazzo. *Int. J. Quantum Chem.* **2016**, *116*, 1575–1602. DOI: 10.1002/qua.25192

REFERENCES

[1] G. A. Somorjai, *Introduction to Surface Chemistry and Catalysis*, *Wiley*, ***1994***. *Hoboken, New Jersey, U.S.*

[2] D. A. Williams, E. Herbst, *Surf. Sci.* **2002**, *500*, 823.

[3] M. I. Katsnelson, M. I. Katsnelson, *Graphene: Carbon in Two Dimensions*, *Cambridge University Press*, ***2012***. *ISBN 978-0-521-19540-9. Cambridge.*

[4] M. Aliofkhazraei, N. Ali, W. I. Milne, C. S. Ozkan, S. Mitura, J. L. Gervasoni, Eds., *Graphene Science Handbook, Six-Volume Set*, *CRC Press*, ***2016***. *ISBN 978-1-4665-9118-9. Boca Raton, FL, U.S.*

[5] J. Harris, in *Dynamics of gas-Surface Interactions (Eds: Rettner C. T., Ashfold M. N. R.), p. 6-46. The Royal Society of Chemistry*, ***1991***. *Letchworth, U.K.*

[6] R. W. Zwanzig, *J. Chem. Phys.* **1960**, *32*, 1173.

[7] S. A. Adelman, J. D. Doll, *J. Chem. Phys.* **1976**, *64*, 2375.

[8] H. F. Winters, H. Coufal, C. T. Rettner, D. S. Bethune, *Phys. Rev. B* **1990**, *41*, 6240.

[9] E. K. Grimmelmann, J. C. Tully, M. J. Cardillo, *J. Chem. Phys.* **1980**, *72*, 1039.

[10] K. Golibrzuch, P. R. Shirhatti, J. Altschäffel, I. Rahinov, D. J. Auerbach, A. M. Wodtke, C. Bartels, *J. Phys. Chem. A* **2013**, *117*, 8750.

[11] B. Jackson, F. Nattino, G. J. Kroes, *J. Chem. Phys.* **2014**, *141*, 054102.

[12] R. W. Fuller, S. M. Harris, E. L. Slaggie, *Am. J. Phys.* **1963**, *31*, 431.

[13] M. Sunjic, A. A. Lucas, *Phys. Rev. B* **1971**, *3*, 719.

[14] D. P. Craig, T. Thirunamachandran, *Molecular Quantum Electrodynamics: An Introduction to Radiation–Molecule Interactions*, *Dover Publications*, *1998*, *Mineola, N.Y., U.S.*,

[15] H. Nienhaus, *Surf. Sci. Rep.* **2002**, *45*, 1.

[16] H. Metiu, J. W. Gadzuk, *J. Chem. Phys.* **1981**, *74*, 2641.

[17] Y. Huang, A. M. Wodtke, H. Hou, C. T. Rettner, D. J. Auerbach, *Phys. Rev. Lett.* **2000**, *84*, 2985.

[18] Y. Huang, C. T. Rettner, D. J. Auerbach, A. M. Wodtke, *Science* **2000**, *290*, 111.

[19] S. Li, H. Guo, *J. Chem. Phys.* **2002**, *117*, 4499.

[20] J. D. White, J. Chen, D. Matsiev, D. J. Auerbach, A. M. Wodtke, *Nature* **2005**, *433*, 503.

[21] G. Katz, Y. Zeiri, R. Kosloff, *J. Phys. Chem. B* **2005**, *109*, 18876.

[22] J. D. White, J. Chen, D. Matsiev, D. J. Auerbach, A. M. Wodtke, *J. Chem. Phys.* **2006**, *124*, 64702. 0

[23] N. Shenvi, S. Roy, J. C. Tully, *J. Chem. Phys.* **2009**, *130*, 174107.

[24] N. Shenvi, S. Roy, J. C. Tully, *Science* **2009**, *326*, 829.

[25] S. Monturet, P. Saalfrank, *Phys. Rev. B* **2010**, *82*, 075404.

[26] K. Golibrzuch, N. Bartels, D. J. Auerbach, A. M. Wodtke, *Annu. Rev. Phys. Chem.* **2015**, *66*, 399.

[27] M. Head-Gordon, J. C. Tully, *J. Chem. Phys.* **1995**, *103*, 10137.

[28] J. D. Jackson, *Classical Electrodynamics*, *Wiley*, ***1998***. *ISBN 978-0-471-30932-1. New York, U.S.*

[29] H. Bethe, *Ann. Phys.* **1930**, *397*, 325.

[30] E. Fermi, E. Teller, *Phys. Rev.* **1947**, *72*, 399.

[31] T. L. Ferrell, R. H. Ritchie, *Phys. Rev. B* **1977**, *16*, 115.

[32] P. M. Echenique, R. M. Nieminen, R. H. Ritchie, *Solid State Commun.* **1981**, *37*, 779.

[33] P. M. Echenique, R. M. Nieminen, J. C. Ashley, R. H. Ritchie, *Phys. Rev. A* **1986**, *33*, 897.

[34] J. I. Juaristi, M. Alducin, R. D. Muiño, H. F. Busnengo, A. Salin, *Phys. Rev. Lett.* **2008**, *100*, 116102.

[35] M. Blanco-Rey, J. Juaristi, R. Díez Muiño, H. Busnengo, G. Kroes, M. Alducin, *Phys. Rev. Lett.* **2014**, *112*, 103203.

[36] M. Bonfanti, B. Jackson, K. H. Hughes, I. Burghardt, R. Martinazzo, *J. Chem. Phys.* **2015**, *143*, 124704.

[37] J. V. Barth, *Surf. Sci. Rep.* **2000**, *40*, 75.

[38] F. Reif, *Fundamentals of Statistical and Thermal Physics*, *McGraw-Hill*, ***1965***. *New York, U.S.*

[39] R. Morgado, F. A. Oliveira, G. G. Batrouni, A. Hansen, *Phys. Rev. Lett.* **2002**, *89*, 100601.

[40] R. Kubo, M. Toda, N. Hashitsume, *Statistical Physics II—Nonequilibrium Statistical Mechanics*, *Springer Series in Solid-State Sciences.*, *Vol.* 31, *Springer Verlag*, ***1991***. *Berlin, Germany*.

[41] U. Weiss, *Quantum Dissipative Systems*, *3rd ed.*, *World Scientific*, *Singapore*, ***2008***.

[42] H. A. Kramers, *Physica* **1940**, *7*, 284.

[43] P. Hänggi, P. Talkner, M. Borkovec, *Rev. Mod. Phys.* **1990**, *62*, 251.

[44] E. Pollak, *J. Chem. Phys.* **1986**, *85*, 865.

[45] E. Pollak, *Chem. Phys. Lett.* **1986**, *127*, 178.

[46] A. Nitzan, *Chemical Dynamics in Condensed Phases—Relaxation, Transfer and Reactions in Condensed Molecular Systems*, *Oxford Graduate Texts*, *Oxford University Press*, ***2006***. *ISBN 978019852979. Oxford, U.K.*

[47] M. Bonfanti, K. H. Hughes, I. Burghardt, R. Martinazzo, *Ann. Phys.* **2015**, *527*, 556.

[48] K. H. Hughes, C. D. Christ, I. Burghardt, *J. Chem. Phys.* **2009**, *131*, 024109.

[49] K. H. Hughes, C. D. Christ, I. Burghardt, *J. Chem. Phys.* **2009**, *131*, 124108.

[50] R. Martinazzo, B. Vacchini, K. H. Hughes, I. Burghardt, *J. Chem. Phys.* **2011**, *134*, 011101.

[51] R. Martinazzo, K. H. Hughes, I. Burghardt, *Phys. Rev. E* **2011**, *84*, 030102.

[52] C. T. Rettner, *Phys. Rev. Lett.* **1992**, *69*, 383.

[53] C. T. Rettner, D. J. Auerbach, *Phys. Rev. Lett.* **1995**, *74*, 4551.

[54] C. T. Rettner, D. J. Auerbach, *Surf. Sci.* **1996**, *602*, 357.

[55] C. T. Rettner, D. J. Auerbach, *J. Chem. Phys.* **1996**, *104*, 2732.

[56] C. T. Rettner, *J. Chem. Phys.* **1994**, *101*, 1529.

[57] B. Jackson, D. Lemoine, *J. Chem. Phys.* **2001**, *114*, 474.

[58] M. Pasquini, M. Bonfanti, R. Martinazzo, *Phys. Chem. Chem. Phys.* **2016**, *18*, 6607.

[59] R. D. Levine, R. B. Bernstein, *Molecular Reaction Dynamics and Chemical Reactivity*, *Oxford University Press*, ***1987***. *Oxford, U.K.*

[60] J. Harris, B. Kasemo, *Surf. Sci.* **1981**, *105*, L281.

[61] D. V. Shalashilin, B. Jackson, *J. Chem. Phys.* **1998**, *108*, 2856.

[62] G. R. Darling, S. Holloway, *Rep. Prog. Phys.* **1995**, *58*, 1595.

[63] A. Gross, *Surf. Sci. Rep.* **1998**, *32*, 291.

[64] G. J. Kroes, *Prog. Surf. Sci.* **1999**, *60*, 1.

[65] G. J. Kroes, M. F. Somers, *J. Theor. Comput. Chem.* **2005**, *4*, 493.

[66] A. C. Luntz, J. Harris, *Surf. Sci.* **1991**, *258*, 397.

[67] M. Dohle, P. Saalfrank, *Surf. Sci.* **1997**, *373*, 95.

[68] H. F. Busnengo, W. Dong, P. Sautet, A. Salin, *Phys. Rev. Lett.* **2001**, *87*, 127601.

[69] C. Díaz, R. A. Olsen, D. J. Auerbach, G. J. Kroes, *Phys. Chem. Chem. Phys.* **2010**, *12*, 6499.

[70] J. M. Bowman, *Int. J. Quant. Chem.* **1979**, *16*, 487.

[71] J. M. Bowman, G. Drolshagen, J. P. Toennies, *J. Chem. Phys.* **1979**, *71*, 2270.

[72] M. Wijzenbroek, M. F. Somers, *J. Chem. Phys.* **2012**, *137*, 054703.

[73] R. Martinazzo, S. Assoni, G. Marinoni, G. F. Tantardini, *J. Chem. Phys.* **2004**, *120*, 8761.

[74] T. N. Truong, D. G. Truhlar, B. C. Garrett, *J. Phys. Chem.* **1989**, *93*, 8227.

[75] M. S. Daw, M. I. Baskes, *Phys. Rev. Lett.* **1983**, *50*, 1285.

[76] M. S. Daw, M. I. Baskes, *Phys. Rev. B* **1984**, *29*, 6443.

[77] F. Nattino, D. Migliorini, M. Bonfanti, G. J. Kroes, *J. Chem. Phys.* **2016**, *144*, 044702.

[78] S. Casolo, G. F. Tantardini, R. Martinazzo, *Proc. Natl. Acad. Sci. U. S. A.* **2013**, *110*, 6674.

[79] S. Casolo, G. F. Tantardini, R. Martinazzo, *J. Phys. Chem. A*, in press. DOI: 10.1021/acs.jpca.5b12761

[80] M. Persson, B. Jackson, *J. Chem. Phys.* **1995**, *102*, 1078.

[81] X. Sha, B. Jackson, *Surf. Sci.* **2002**, *496*, 318.

[82] X. Sha, B. Jackson, D. Lemoine, *J. Chem. Phys.* **2002**, *116*, 7158.

[83] R. Martinazzo, G. F. Tantardini, *J. Chem. Phys.* **2005**, *122*, 094109.

[84] S. Casolo, R. Martinazzo, M. Bonfanti, G. F. Tantardini, *J. Phys. Chem. A* **2009**, *113*, 14545.

[85] R. Martinazzo, G. F. Tantardini, *J. Chem. Phys.* **2006**, *124*, 124702.

[86] R. Martinazzo, G. F. Tantardini, *J. Chem. Phys.* **2006**, *124*, 124703.

[87] M. Bonfanti, S. Casolo, G. F. Tantardini, R. Martinazzo, *Phys. Chem. Chem. Phys.* **2011**, *13*, 16680.

[88] R. Martinazzo, S. Casolo, L. H. Hornekaer, in *Dynamics of Gas-Surface Interactions (Eds: R. Díez Muiño, H. F. Busnengo)*, *no. 50*, *Springer Series in Surface Sciences*, *pp. 157–177*, *Springer, Berlin, Heidelberg*, ***2013***. *ISBN 978-3-642-32954-8 978-3-642-32955-5, dOI: 10.1007/978-3-642-32955-5_7*.

[89] M. Bonfanti, M. F. Somers, C. Díaz, H. F. Busnengo, G. J. Kroes, Z. *Phys. Chem.* **2013**, *227*, 1397.

[90] I. Andrianov, P. Saalfrank, *J. Chem. Phys.* **2006**, *124*, 034710.

[91] F. Lüder, M. Nest, P. Saalfrank, *Theor. Chem. Acc.* **2010**, *127*, 183.

[92] H. D. Meyer, U. Manthe, L. S. Cederbaum, *Chem. Phys. Lett.* **1990**, *165*, 73.

[93] M. H. Beck, A. Jäckle, G. A. Worth, H. D. Meyer, *Phys. Rep.* **2000**, *324*, 1.

[94] H. D. Meyer, F. Gatti, G. A. Worth (Eds.), *Multidimensional Quantum Dynamics: MCTDH Theory and Applications*, *Wiley, VCH Verlag GmbH & Co. KGaA, Weinheim*, ***2009***.

[95] M. Nest, R. Kosloff, *J. Chem. Phys.* **2007**, *127*, 134711.

[96] M. Bonfanti, B. Jackson, K. H. Hughes, I. Burghardt, R. Martinazzo, *J. Chem. Phys.* **2015**, *143*, 124703.

[97] G. W. Ford, J. T. Lewis, R. F. O'Connell, *Phys. Rev. A* **1988**, *37*, 4419.

[98] N. Pottier, *Nonequilibrium Statistical Physics: Linear Irreversible Processes*, *Oxford Graduate Texts*, *Oxford University Press*, ***2010***, *ISBN 9780199556885. Oxford, U.K.*

[99] A. O. Caldeira, A. J. Leggett, *Phys. Rev. Lett.* **1981**, *46*, 211.

[100] A. O. Caldeira, and A. J. Leggett, (**1983**). Quantum Tunnelling in a Dissipative System. *Annals of Physics 149*: 374. doi:10.1016/0003-4916(83)90202-6.